POLITECNICO DI TORINO
Repository ISTITUZIONALE

Spatial and temporal distributions of U.S. winds and wind power at 80 m derived from measurements

*Original*
Spatial and temporal distributions of U.S. winds and wind power at 80 m derived from measurements / Lozej Archer, C., Jacobson, M.Z.. - In: JOURNAL OF GEOPHYSICAL RESEARCH. - ISSN 0148-0227. - 108:9(2003). [10.1029/2002jd002076]

*Availability:*
This version is available at: 11583/3010494 since: 2026-05-02T13:29:24Z

*Publisher:*
AGU Publications

*Published*
DOI:10.1029/2002jd002076

*Terms of use:*

This article is made available under terms and conditions as specified in the corresponding bibliographic description in the repository

*Publisher copyright*

(Article begins on next page)

07 November 2026

JOURNAL OF GEOPHYSICAL RESEARCH, VOL. 108, NO. D9, 4289, doi:10.1029/2002JD002076, 2003

***Correction published 29 October 2004***

# Spatial and temporal distributions of U.S. winds and wind power at 80 m derived from measurements

Cristina L. Archer and Mark Z. Jacobson

Department of Civil and Environmental Engineering, Stanford University, Stanford, California, USA

Received 9 January 2002; revised 14 December 2002; accepted 20 December 2002; published 13 May 2003.

[1] This is a study to quantify U.S. wind power at 80 m (the hub height of large wind turbines) and to investigate whether winds from a network of farms can provide a steady and reliable source of electric power. Data from 1327 surface stations and 87 soundings in the United States for the year 2000 were used. Several methods were tested to extrapolate 10-m wind measurements to 80 m. The most accurate, a least squares fit based on twice-a-day wind profiles from the soundings, resulted in 80-m wind speeds that are, on average, 1.3–1.7 m/s faster than those obtained from the most common methods previously used to obtain elevated data for U.S. wind power maps, a logarithmic law and a power law, both with constant coefficients. The results suggest that U.S. wind power at 80 m may be substantially greater than previously estimated. It was found that 24% of all stations (and 37% of all coastal/offshore stations) are characterized by mean annual speeds $\geq$6.9 m/s at 80 m, implying that the winds over possibly one quarter of the United States are strong enough to provide electric power at a direct cost equal to that of a new natural gas or coal power plant. The greatest previously uncharted reservoir of wind power in the continental United States is offshore and nearshore along the southeastern and southern coasts. When multiple wind sites are considered, the number of days with no wind power and the standard deviation of the wind speed, integrated across all sites, are substantially reduced in comparison with when one wind site is considered. Therefore a network of wind farms in locations with high annual mean wind speeds may provide a reliable and abundant source of electric power. *INDEX TERMS:* 0345 Atmospheric Composition and Structure: Pollution—urban and regional (0305); 3399 Meteorology and Atmospheric Dynamics: General or miscellaneous; 9350 Information Related to Geographic Region: North America; *KEYWORDS:* U.S. wind power, least squares, global warming, air pollution, energy, wind speed

**Citation:** Archer, C. L., and M. Z. Jacobson, Spatial and temporal distributions of U.S. winds and wind power at 80 m derived from measurements, *J. Geophys. Res.*, *108*(D9), 4289, doi:10.1029/2002JD002076, 2003.

## 1. Introduction

[2] In 1999, coal (50.8%) and natural gas (15.4%) generated about 66.2% of electric power in the United States. Wind generated only 0.12% of electric power [*Energy Information Administration* (*EIA*), 2001] (available at http://www.eia.doe.gov/cneaf/electricity/epav2/epav2t1.txt).

[3] The direct cost of energy from a large (1.5 MW, 77-m blade) modern wind turbine in the presence of mean annual Rayleigh-distributed winds of speed 7–7.5 m/s appears to have decreased to 2.9–3.9 cents/kWh [*Jacobson and Masters*, 2001; *Bolinger and Wiser*, 2001]. This compares with 3.5–4 cents/kWh from a new pulverized coal-fired power plant and 3.3–3.6 cents/kWh from a new natural gas combined cycle power plant [*Office of Fossil Energy*, 2001] (available at http://www.fe.doe.gov/coal_power/special_rpts/market_systems/market_sys.html). The one-tail Rayleigh wind speed distribution is often used for calculating wind speed statistics and will be discussed in detail in section 2.4.

Copyright 2003 by the American Geophysical Union.
0148-0227/03/2002JD002076

[4] Coal and natural gas both emit $CO_2$, $CH_4$, $SO_2$, $NO_x$, CO, $NH_3$, reactive organic gases, particulate black carbon, particulate organic matter, and other particulate components. The emissions from coal and natural gas enhance global warming, respiratory and cardiovascular disease, air-pollution-related mortality, urban smog, acid deposition, and visibility degradation. Coal mining also results in black-lung disease, land-surface stripping, water pollution, and mercury emissions. Wind energy causes no air pollution past the manufacturing and scrapping process.

[5] Despite the relatively even direct cost of new wind turbines versus new coal and natural gas power plants, subsidies to both, and the high health/environmental costs of coal and natural gas versus wind, many still argue that an advantage of coal and natural gas power plants is that they are more reliable sources of energy because winds are intermittent. They argue that the intermittency results in two costs. The first is the cost of "regulation ancillary service," which is the cost incurred when grid operators must instantaneously switch to another power source when the first source does not produce power temporarily. *Hirst* [2001] (available at http://www.EHirst.com/PDF/

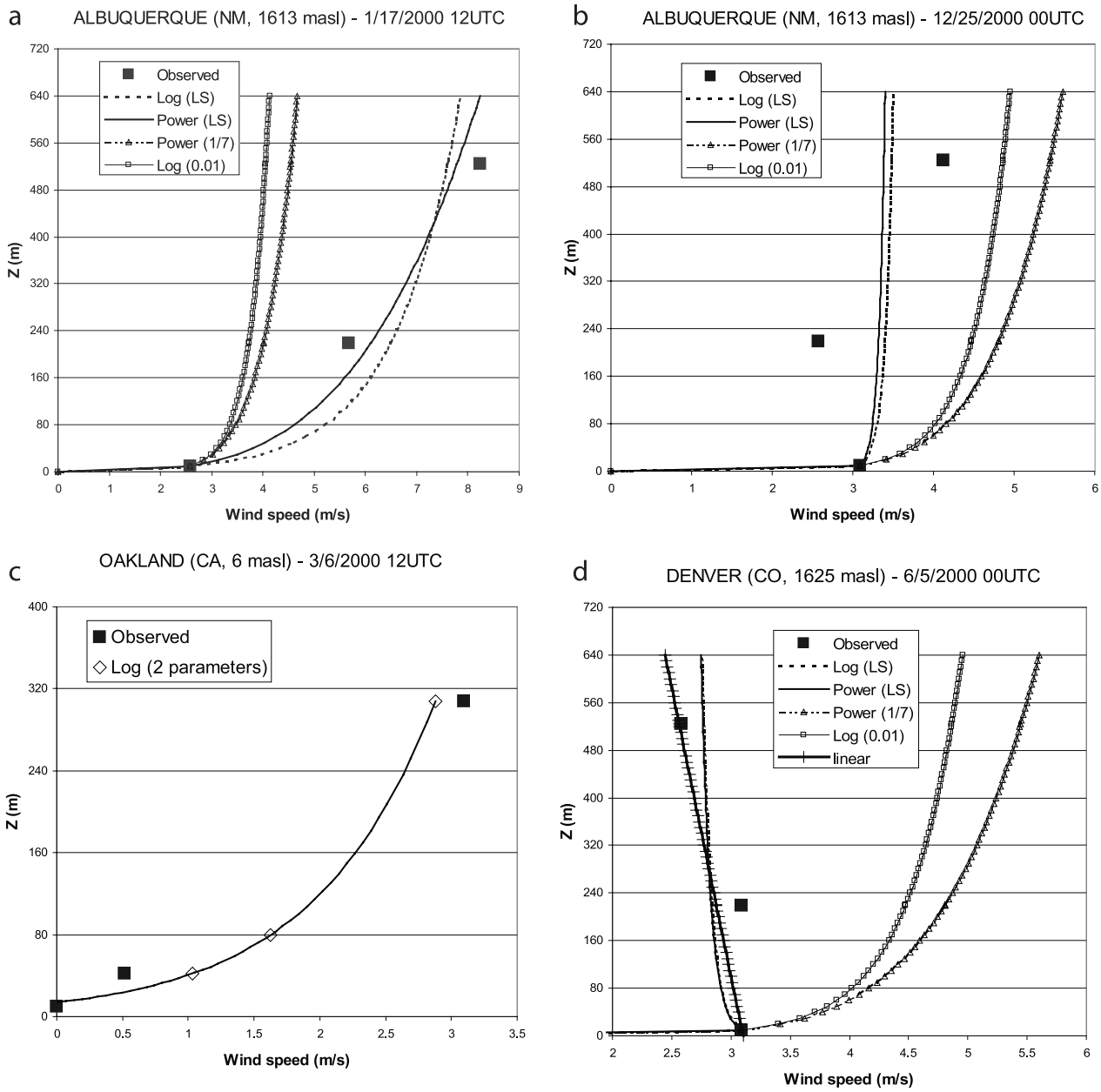


**Figure 1.** (a–d) Observed (large filled squares) and interpolated profiles of wind speed (triangles: power law with 1/7 friction coefficient; squares: logarithmic law with 0.01 roughness length; solid line: power law with LS friction coefficient; dashed line: logarithmic law with LS roughness length; diamonds: 2-parameter logarithmic law; thick line with "+" mark: linear regression) for various sounding locations. The LS power law and the LS logarithmic law curves are indistinguishable in Figure 1d.

WindIntegration.pdf), and *Hudson et al.* [2001] showed that this cost is relatively trivial, 0.005 to 0.030 cents/kWh (<1% the direct cost of wind energy), when wind is a small fraction of the total energy supply. The second is the cost of maintaining and using backup (contingency) reserves (usually in the form of "peaker" fossil-fuel power plants) when wind is a large fraction (e.g., 30%) of the total energy supply and wind's output is low for a given hour.

[6] The real issue in the second case is not the intermittency cost to wind, if any, but the difference between the intermittency cost to wind and that to coal or natural gas. Coal and natural gas have their own intermittency problems. For example, the forced outage rate of fossil-fuel power plants is about 8% [*North American Electric Reliability Council*, 2000], whereas the forced plus unforced outage rate of modern turbines is about 2% (Danish Windturbine Manufacturers Association, 21 frequently asked questions about wind energy, updated 16 April 2001, available at http://www.windpower.dk/faqs.htm). In addition, the variation of natural gas supplies results in monthly to yearly price fluctuations of electric power of 50–100% (T. McFeat, The unnatural price of natural gas, CBC News Online, Jan. 2001, available at http://www.cbc.ca/news/indepth/background/gas_hikes.html).

215622024, 2003, D9, Downloaded from https://agupubs.onlinelibrary.wiley.com/doi/10.1029/2002JD002076 by CochraneItalia, Wiley Online Library on [10/05/2026]. See the Terms and Conditions (https://onlinelibrary.wiley.com/terms-and-conditions) on Wiley Online Library for rules of use; OA articles are governed by the applicable Creative Commons License

215622020, 2003, D9, Downloaded from https://agupubs.onlinelibrary.wiley.com/doi/10.1029/2002JD002076 by CochraneItalia, Wiley Online Library on [10/05/2026]. See the Terms and Conditions (https://onlinelibrary.wiley.com/terms-and-conditions) on Wiley Online Library for rules of use; OA articles are governed by the applicable Creative Commons License

**Table 1.** Location and Elevations at the 16 Sites Selected by *Sandusky et al.* [1982]

| Site Location | Lower Level, m | Middle Level, m | Upper Level, m |
|---|---|---|---|
| Augspurger Mt. (WA) | 9.1 | – | 45.7 |
| Amarillo (TX) | 9.1 | – | 45.7 |
| Block Island (RI) | 9.1 | 30.0 | 45.7 |
| Boardman (OR) | 9.1 | 39.6 | 70.1 |
| Boone (NC) | 18.2 | 45.7 | 76.2 |
| Clayton (NM) | 9.1 | 30.0 | 45.7 |
| Cold Bay (AK) | 9.1 | – | 21.8 |
| Culebra (PR) | 9.1 | – | 45.7 |
| Holyoke (MA) | 18.2 | – | 45.7 |
| Huron (SD) | 9.1 | – | 45.7 |
| Kingsley Dam (NE) | 9.1 | – | 45.7 |
| Ludington (MI) | 18.2 | – | 45.7 |
| Montaulk (NY) | 18.2 | – | 45.7 |
| Point Arena (CA) | 9.1 | – | 45.7 |
| Russell (KS) | 9.1 | – | 45.7 |
| San Gorgonio (CA) | 9.1 | 30.0 | 45.7 |

[7] In addition, even though contingency reserves may be required for wind, they do not always need to result in an extra cost. For example, one source of contingency reserves is hydroelectric power, which supplies about 10% of the electric power in the United States (mostly in California, Oregon, and Washington). This source does not incur a cost if its output must be increased on short notice. Additional hydroelectric power used when wind power is low can be balanced by less hydroelectric power used when wind power is high, stabilizing the summed energy supplied by hydroelectric power and wind.

[8] Finally, if wind becomes 30% of the energy supply, wind farms would be distributed over greater areas, and grid interconnections would expand, enabling easier transmission of excess wind, solar, hydroelectric, fossil, and nuclear energy from outside the local grid to the local grid, thereby reducing the need for contingency reserves. Yet, the main issue that has not been resolved is whether wind's instantaneous intermittency at a given location translates into intermittency of hourly-averaged electric power, summed over wind farms on a larger scale. If, indeed, wind can provide a stable amount of electric power when all turbines over a large number of farms are considered, then backup requirements and associated costs can be minimized.

[9] For this study, wind data from the United States for the year 2000 were used to examine whether a large network of wind farms can provide electric power more or less reliably than a small network or a single farm. The paper also provides an analysis of the time of peak wind production during the day, a map of the mean-annual wind speeds at 80 m at all wind measurement sites in the United States for the year 2000, an analysis of the Rayleigh nature of wind speeds, and other wind-related statistics.

## 2. Methodology

[10] For this study, year 2000 wind speed data from NCDC [*National Climatic Data Center*, 2001] and FSL (Forecast Systems Laboratory, Radiosonde data archive, 2001, available at http://raob.fsl.noaa.gov/) were used to generate maps and statistics to examine U.S. wind power. Two types of data were considered: surface measurements from 1327 stations and sounding measurements from 87 stations. Sounding measurements were generally available at "mandatory levels," i.e., vertical levels characterized by prescribed atmospheric pressures. Typical mandatory levels were 1000, 950, 925, 900, 800 mb, etc. Depending on station altitude and weather conditions, the elevations of some of these levels varied. Approximately 20% of the sounding stations reported measurements at an elevation of 80 m ± 20 m (i.e., between 60 and 100 m above the ground). Surface stations provide wind speed measurements only at a standard elevation of 10 m above the ground (sometimes at a non-standard elevation of 20 feet). In the next sections, a new methodology of interpolating sounding data and extrapolating surface data to 80 m (the hub height of modern, large turbines) is developed.

### 2.1. Methodology for 80-m Wind Speed Determination

[11] Two approaches are commonly used to extrapolate 10-m wind speed data to 80-m. The first one is the power-law relation [e.g., *Elliott et al.*, 1986; *Arya*, 1988] (the former is available at http://rredc.nrel.gov/wind/pubs/atlas),

$$V(z) = V_R\left(\frac{z}{z_R}\right)^{\alpha} \tag{1}$$

where $V(z)$ is wind speed at elevation $z$ above the topographical surface (80 m in this case, i.e., $V(80)$), $V_R$ is wind speed at the reference elevation $z_R$ (10 m above the topographical surface in the rest of this paper), and $\alpha$ (typically 1/7) is the friction coefficient. The second one is the logarithmic law [e.g., *Arya*, 1988; *Jacobson*, 1999],

$$V(z) = V_R\frac{\ln\left(\frac{z}{z_0}\right)}{\ln\left(\frac{z_R}{z_0}\right)} \tag{2}$$

where $z_0$ (typically 0.01 m) is the roughness length. Note that both curves must pass through $V_R$ (i.e., at $z = z_R = 10$ m, they return the value $V(10) = V_R$) and they both require one fitting parameter, either $\alpha$ or $z_0$. The logarithmic law is theoretically valid for neutral atmospheric conditions only (i.e., when vertical motions are neither inhibited nor supported by the atmosphere). It can be obtained by similarity theory after assuming no Coriolis effect and a flat, uniform surface [*Arya*, 1988]. The power law does not have a theoretical basis, but it often provides a reasonable fit to observed vertical wind profiles [*Arya*, 1988]. The advantage of these two approaches is their simplicity (only one, constant parameter is required). However, atmospheric conditions are rarely neutral and diurnal, seasonal or stability-dependant variations cannot be taken into account by using one constant parameter.

[12] Given these limitations, a new methodology of extrapolating wind speed above a surface station measure-

**Table 2.** Wind Speeds Corresponding to Different Power Classes at 10 m and 80 m

| Class | Wind Speed at 10 m, m/s | Wind Speed at 80 m, m/s |
|---|---|---|
| 1 | <4.4 | <5.9 |
| 2 | 4.4–5.1 | 5.9–6.9 |
| 3 | 5.1–5.6 | 6.9–7.5 |
| 4 | 5.6–6.0 | 7.5–8.1 |
| 5 | 6.0–6.4 | 8.1–8.6 |
| 6 | 6.4–7.0 | 8.6–9.4 |
| 7 | >7.0 | ≥9.4 |

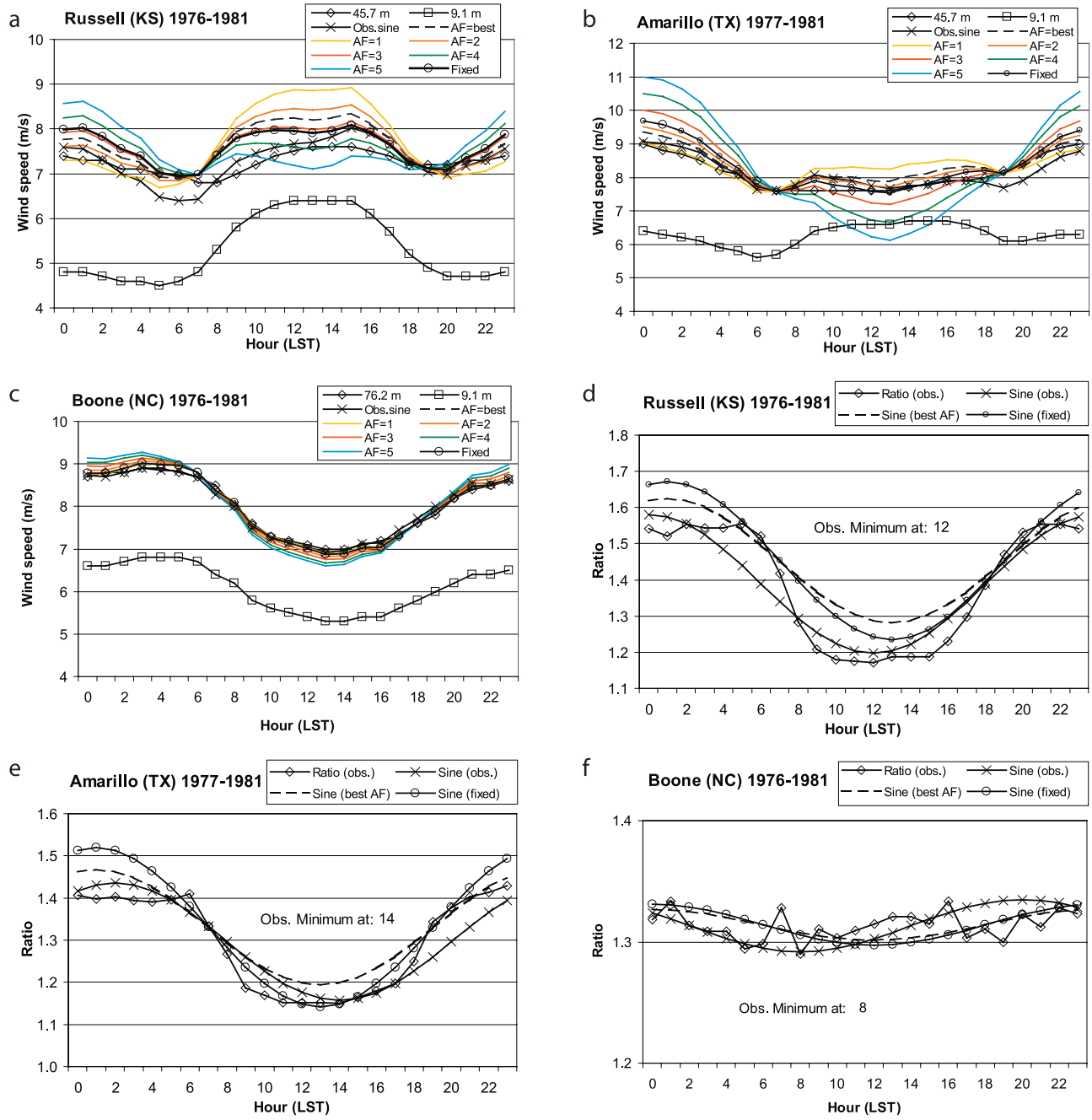


**Figure 2.** (a–f) Examples of application of the hourly trend methodology (described in section 2.2) to three sites of the data set of *Sandusky et al.* [1982]: Russell (KS) and Amarillo (TX), with measurements at 9 and 45 m, and Boone (NC), with measurements at 9 and 76 m. Figures 2a–2c show the hourly trend of 80-m wind speed, observed (diamonds) and extrapolated after assuming different sine curves: with observed parameters in equation (10) (crosses), with minimum at fixed time (1300) and amplification factor fixed to 1.2 (circles), with minimum at fixed time (1300) and amplification factor giving the lowest total error (dashed), and several similar sine curves with minimum at fixed time (1300) and various values of the amplification factor (color-coded). Figures 2d–2f show the observed (diamonds) ratio ρ and several sine curves corresponding to the above assumptions.

ment was developed. The methodology is referred to here as the least squares fitting approach (LS hereafter), and it involves three steps:

[13] 1. For each sounding station, four fitting parameters are calculated for each hour (typically at 0000 and 1200 UTC) of each day to reproduce empirically the wind speed variation with height at the sounding. Of the four parameters, the "best" fitting parameter, calculated as the one giving the lowest residual (described shortly) is saved.

[14] 2. For each surface station, the five nearest-in-space sounding stations are selected. Then, $V_R$ from the surface station and the "best" fitting parameter from each sounding

21562202d, 2003, D9, Downloaded from https://agupubs.onlinelibrary.wiley.com/doi/10.1029/2002JD002076 by CochraneItalia, Wiley Online Library on [10/05/2026]. See the Terms and Conditions (https://onlinelibrary.wiley.com/terms-and-conditions) on Wiley Online Library for rules of use; OA articles are governed by the applicable Creative Commons License

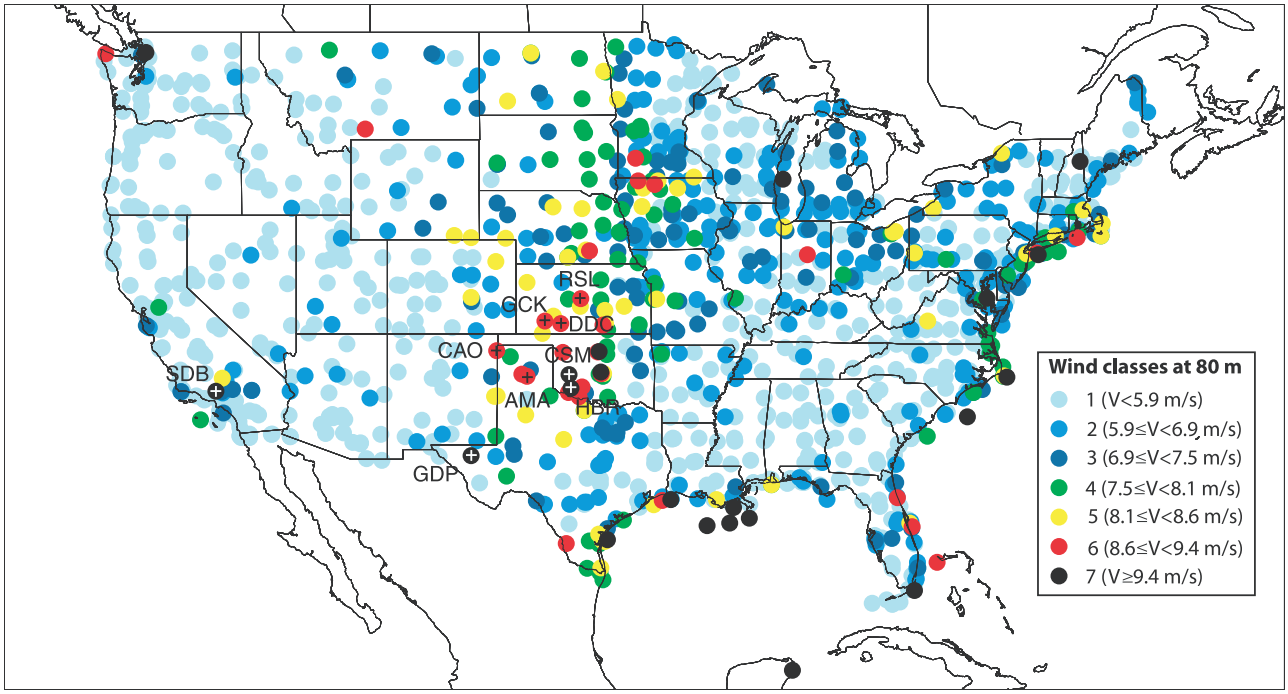


**Figure 3.** Map of wind speed extrapolated to 80 m, averaged over all hours of the year 2000, for the continental United States, obtained as described in the text. The 10 stations selected for additional statistics are marked with a plus sign. The map gives speeds only at the specific locations where measurements were taken.

station are used to calculate a new $V(80)$ at each of the five sounding stations. Note that the average distance between sounding stations in the contiguous United States is approximately 300 km [*Steurer*, 1996].

[15] 3. Finally, $V(80)$ at the surface station is calculated as the weighted average of the five new $V(80)$s from the sounding stations, where the weighting is the inverse square of the distance between the surface station and each sounding station.

[16] The four fitting parameters for each hour of available data (typically twice a day) at each sounding station were determined as follows. An equation for the residual $R$ of the squares of the error in wind speed was written as

$$R = \sum_{i=1}^{N} [V_i - V(z_i)]^2, \tag{3}$$

where $N$ is a selected number of points in the bottom part of a sounding (N = 3 in this case), $V_i$ is the wind speed observed at vertical point $i$ in the sounding (the first vertical point is at 10 m, i.e., $z_1 = z_R = 10$ m), and $V(z_i)$ is the wind speed calculated by one of several possible equations, such as equations (1) or (2). Setting the partial derivative of $R$ with respect to the fitting parameter in equations (1) and (2) ($\alpha$ and $z_0$, respectively) to zero and solving for the fitting parameter gives two LS fitting parameters,

$$\alpha^{LS} = \frac{\sum_{i=1}^{N} \ln\left(\frac{V_i}{V_R}\right) \ln\left(\frac{z_i}{z_R}\right)}{\sum_{i=1}^{N} \ln\left(\frac{z_i}{z_R}\right)^2} \tag{4}$$

$$\ln\left(z_0^{LS}\right) = \frac{V_R\left\{\sum_{i=1}^{N}[\ln(z_i)]^2 - \ln(z_R)\sum_{i=1}^{N}\ln(z_i)\right\} - \ln(z_R)\sum_{i=1}^{N}\left(V_i \ln\left(\frac{z_i}{z_R}\right)\right)}{\left\{V_R\sum_{i=1}^{N}\ln(z_i) - \sum_{i=1}^{N}\left[V_i \ln\left(\frac{z_i}{z_R}\right)\right] - NV_R\ln(z_R)\right\}}. \tag{5}$$

[17] Note that $\alpha$ and $z_0$, acquire different values for each observed wind profile. Figures 1a and 1b show an example of curves interpolated with LS parameters obtained from equation (4) and equation (5) for N = 3. For comparison, curves with $\alpha$ = 1/7 and $z_0$ = 0.01 m are plotted too. In this study, curves with $\alpha$ = 1/7 and $z_0$ = 0.01 m underestimated the value of $V(80)$ (as in Figure 1a) in about 60% of the cases tested, but the opposite occurred in less than 40% of the cases (e.g., Figure 1b). The power law with $\alpha$ = 1/7 led to an average underestimate of annual mean 80-m wind speed of 1.3 m/s. The logarithmic law with $z_0$ = 0.01 m underestimated the annual mean 80-m wind speed by 1.7 m/s on average. Both the power law with $\alpha$ = 1/7 and the logarithmic law with $z_0$ = 0.01 m led to greater underestimates at night (i.e., 1200 UTC) than during the day (i.e., 0000 UTC), averaging 2.5 and 2.8 m/s (respectively) below the LS mean 80-m wind speed at night, and 0.1 and 0.5 m/s (respectively) during the day.

[18] Some unusual weather conditions cause wind speed either to decrease with height (Figure 1d) or to be zero at 10 m (Figure 1c). For these special cases, the two remaining fitting parameters were determined.

[19] Since equation (1) and equation (2) have $V_R$ as a multiplying factor, they unrealistically predict zero wind speed for all vertical points when $V_R = 0$. The solution is to use a two-parameter logarithmic law of the form

215622024, 2003, D9, Downloaded from https://agupubs.onlinelibrary.wiley.com/doi/10.1029/2002JD002076 by CochraneItalia, Wiley Online Library on [10/05/2026]. See the Terms and Conditions (https://onlinelibrary.wiley.com/terms-and-conditions) on Wiley Online Library for rules of use; OA articles are governed by the applicable Creative Commons License

**Table 3.** U.S. States With the Highest Number of Stations in Classes ≥3 at 80 m, With Emphasis on the Number of Offshore/Coastal Sites

| State | Total Number of Stations | Number of Class ≥3 Stations | Percent of Class ≥3 Stations | Number of Coastal/Offshore Stations | Number of Coastal/Offshore Class ≥3 Stations | Percent of Coastal/Offshore Class ≥3 Stations | Percent of Class ≥3 Stations That Are Coastal/Offshore |
|---|---|---|---|---|---|---|---|
| Texas | 83 | 35 | 42.2 | 9 | 8 | 88.9 | 22.9 |
| Alaska | 120 | 33 | 27.5 | 44 | 18 | 40.9 | 54.5 |
| Kansas | 29 | 24 | 82.8 | 0 | 0 | 0 | 0 |
| Nebraska | 29 | 23 | 79.3 | 0 | 0 | 0 | 0 |
| Minnesota | 64 | 20 | 31.3 | 0 | 0 | 0 | 0 |
| Oklahoma | 23 | 20 | 87.0 | 0 | 0 | 0 | 0 |
| Iowa | 46 | 18 | 39.1 | 0 | 0 | 0 | 0 |
| Florida | 65 | 11 | 16.9 | 37 | 7 | 18.9 | 63.6 |
| South Dakota | 15 | 13 | 86.7 | 0 | 0 | 0 | 0 |
| California | 101 | 10 | 9.9 | 21 | 4 | 19.0 | 40.0 |
| New York | 34 | 9 | 26.5 | 7 | 4 | 57.1 | 44.4 |
| Ohio | 24 | 10 | 41.7 | 0 | 0 | 0 | 0 |
| Missouri | 20 | 9 | 45.0 | 0 | 0 | 0 | 0 |
| North Dakota | 11 | 9 | 81.8 | 0 | 0 | 0 | 0 |
| North Carolina | 29 | 8 | 27.6 | 10 | 6 | 60.0 | 75.0 |
| Louisiana | 26 | 6 | 23.1 | 8 | 4 | 50.0 | 66.7 |
| Virginia | 37 | 8 | 21.6 | 7 | 4 | 57.1 | 50.0 |
| Massachusetts | 20 | 6 | 30.0 | 8 | 4 | 50.0 | 66.7 |
| Connecticut | 8 | 3 | 37.5 | 3 | 3 | 100 | 100 |
| Hawaii | 19 | 2 | 10.5 | 18 | 2 | 11.1 | 100 |
| New Jersey | 12 | 6 | 50.0 | 3 | 2 | 66.7 | 33.3 |
| Washington | 40 | 3 | 7.5 | 5 | 2 | 40.0 | 66.7 |
| Alabama | 18 | 1 | 5.6 | 2 | 1 | 50.0 | 100 |
| South Carolina | 14 | 1 | 7.1 | 5 | 1 | 20.0 | 100 |
| Maryland | 9 | 2 | 22.2 | 2 | 1 | 50.0 | 50.0 |
| Delaware | 3 | 2 | 66.7 | 2 | 1 | 50.0 | 50.0 |
| Rhode Island | 5 | 2 | 40.0 | 2 | 1 | 50.0 | 50.0 |
| Pacific | 8 | 2 | 25.0 | 8 | 2 | 25.0 | 100 |
| Other states | 502 | 46 | 9.2 | 0 | 0 | 0 | 0 |
| Total United States | 1414 | 342 | 24.2 | 201 | 75 | 37.3 | 21.9 |

$$V_i = A + B^* \ln(z_i), \tag{6}$$

where coefficients A and B, derived by replacing equation (6) in equation (3), are

$$B = \frac{N\sum_{i=1}^{N}[V_i \ln(z_i)] - \sum_{i=1}^{N} V_i \sum_{i=1}^{N} \ln(z_i)}{N\sum_{i=1}^{N}\left[\ln(z_i)^2\right] - \left(\sum_{i=1}^{N} \ln(z_i)\right)^2} \quad A = \frac{\sum_{i=1}^{N} V_i - B\sum_{i=1}^{N} \ln(z_i)}{N}. \tag{7}$$

An example of equation (6) is shown in Figure 1c. Note that the fitting curve obtained with equation (6) is not forced to pass through $V_R$.

[20] If wind speed decreases with height for the lowest N points, then both the power and logarithmic curves show a wrong concavity, due to the fact that either the LS friction coefficient would become negative or the LS roughness length would become too large. In this case, both the 1/7 friction coefficient curve and the 0.01 roughness length curve overestimate $V(80)$ substantially. A solution to this problem is to extrapolate $V(80)$ with a linear regression,

$$V_i = C + D^* z_i, \tag{8}$$

where C and D, obtained from equation (3) by replacing $V_i$ with equation (8), are

$$D = \frac{N\sum_{i=1}^{N}(V_i z_i) - \sum_{i=1}^{N} V_i \sum_{i=1}^{N} z_i}{N\sum_{i=1}^{N}(z_i)^2 - \left(\sum_{i=1}^{N} z_i\right)^2} \qquad C = V_R - D^* z_R. \tag{9}$$

Figure 1d shows an example of this fit. Note that the interpolation line is forced to pass through $V_R$.

[21] In sum, the four fitting parameters calculated for each of the two soundings per day at each sounding station were $\alpha^{LS}$ from equation (4), $z_0{}^{LS}$ from equation (5), A and B from equation (6), C and D from equation (8). The "best" fitting parameter, used for step 1 in the LS procedure, was calculated as the one associated with the lowest residual $R$.

## 2.2. Methodology for Hourly Pattern Determination

[22] At surface stations for which hourly data were available, it was necessary to introduce a methodology for determining the hourly trend of $V(80)$ given only the values calculated at 0000 and 1200 UTC, hereafter referred to as $V_{00}(80)$ and $V_{12}(80)$, obtained with the LS methodology described above. Depending on the time zone of the surface stations, $V_{00}(80)$ and $V_{12}(80)$ were valid within 1500–1900 LST (Local Standard Time) and 0300–0700 LST respectively.

[23] In general, surface (and 10-m) wind speed peaks in the early afternoon, due to the turbulent vertical mixing of horizontal momentum from the upper levels, which is strongest during the afternoon due to the increased thermal instability of the Planetary Boundary Layer (PBL) [*Arya*, 1988; *Riehl*, 1972]. Conversely, at some upper level $z_{rev}$, this trend is reversed, as higher momentum is transferred downward to the surface in the early afternoon by the same mechanism. The elevation of $z_{rev}$ depends on turbulent mixing efficiency, atmospheric thermal stability, and PBL height. It is located at a level far enough from the surface not to be influenced by friction but low enough to be

215622024, 2003, D9, Downloaded from https://agupubs.onlinelibrary.wiley.com/doi/10.1029/2002JD002076 by CochraneItalia, Wiley Online Library on [10/05/2026]. See the Terms and Conditions (https://onlinelibrary.wiley.com/terms-and-conditions) on Wiley Online Library for rules of use; OA articles are governed by the applicable Creative Commons License

21562202d, 2003, D9, Downloaded from https://agupubs.onlinelibrary.wiley.com/doi/10.1029/2002JD002076 by CochraneItalia, Wiley Online Library on [10/05/2026]. See the Terms and Conditions (https://onlinelibrary.wiley.com/terms-and-conditions) on Wiley Online Library for rules of use; OA articles are governed by the applicable Creative Commons License

**Table 4.** Number (and Percent With Respect to Each Region) of U.S. Stations Falling Into Each Wind Power Class at 80 m[a]

| | | Wind Class at 80 m | | | | | | | |
|---|---|---|---|---|---|---|---|---|---|
| | | 1 | 2 | 3 | 4 | 5 | 6 | 7 | ≥3 |
| Region | Total Number | 0 ≤ V < 5.9 m/s | 5.9 ≤ V < 6.9 m/s | 6.9 ≤ V < 7.5 m/s | 7.5 ≤ V < 8.1 m/s | 8.1 ≤ V < 8.6 m/s | 8.6 ≤ V < 9.4 m/s | V ≥ 9.4 m/s | V ≥ 6.9 m/s |
| Northwest | 131 | 105 (80.2) | 14 (10.7) | 6 (4.6) | 1 (0.8) | 2 (1.5) | 2 (1.5) | 1 (0.8) | 12 (9.2) |
| North-Central | 165 | 33 (20.0) | 49 (29.7) | 36 (21.8) | 29 (17.6) | 14 (8.5) | 4 (2.4) | 0 (0.0) | 83 (50.3) |
| Great Lakes | 134 | 56 (41.8) | 49 (36.6) | 21 (15.7) | 3 (2.2) | 3 (2.2) | 1 (0.7) | 1 (0.7) | 29 (21.6) |
| Northeast | 140 | 62 (44.3) | 43 (30.7) | 14 (10.0) | 9 (6.4) | 8 (5.7) | 2 (1.4) | 2 (1.4) | 35 (25.0) |
| East-Central | 114 | 71 (62.3) | 23 (20.2) | 7 (6.1) | 8 (7.0) | 2 (1.8) | 0 (0.0) | 3 (2.6) | 20 (17.5) |
| Southeast | 137 | 98 (71.5) | 26 (19.0) | 6 (4.4) | 1 (0.7) | 2 (1.5) | 3 (2.2) | 1 (0.7) | 13 (9.5) |
| South-Central | 203 | 63 (31.0) | 45 (22.2) | 27 (13.3) | 25 (12.3) | 18 (8.9) | 14 (6.9) | 11 (5.4) | 95 (46.8) |
| Southern Rocky | 105 | 80 (76.2) | 17 (16.2) | 2 (1.9) | 1 (1.0) | 4 (3.8) | 1 (1.0) | 0 (0.0) | 8 (7.6) |
| Southwest | 119 | 100 (84.0) | 9 (7.6) | 6 (5.0) | 2 (1.7) | 1 (0.8) | 0 (0.0) | 1 (0.8) | 10 (8.4) |
| Alaska | 139 | 85 (61.2) | 21 (15.1) | 5 (3.6) | 6 (4.3) | 7 (5.0) | 7 (5.0) | 8 (5.8) | 33 (23.7) |
| Hawaii | 19 | 12 (63.2) | 5 (26.3) | 1 (5.3) | 0 (0.0) | 1 (5.3) | 0 (0.0) | 0 (0.0) | 2 (10.5) |
| Others | 8 | 1 (12.5) | 5 (62.5) | 1 (12.5) | 0 (0.0) | 0 (0.0) | 1 (12.5) | 0 (0.0) | 2 (25.0) |
| United States | 1414 | 766 (54.2) | 306 (21.6) | 132 (9.3) | 85 (6.0) | 62 (4.4) | 35 (2.5) | 28 (2.0) | 342 (24.2) |

[a]Number of stations is given, with percent with respect to each region in parentheses. Stations are grouped into 11 regions as follows: Northwest: Idaho, Montana, Oregon, Washington, Wyoming. North-Central: Nebraska, Iowa, Minnesota, North Dakota, South Dakota. Great Lakes: Illinois, Indiana, Michigan, Ohio, Wisconsin. Northeast: Connecticut, Massachusetts, Rhode Island, Maine, New Hampshire, Vermont, New Jersey, New York, Pennsylvania. East-Central: Delaware, Kentucky, Maryland, North Carolina, Tennessee, Virginia, West Virginia. Southeast: Alabama, Florida, Georgia, Mississippi, South Carolina. South-Central: Arkansas, Kansas, Louisiana, Missouri, Oklahoma, Texas. Southern Rocky: Arizona, Colorado, New Mexico, Utah. Southwest: California, Nevada.

affected by PBL mixing. Without high-resolution sounding data in the vertical and in time, though, it is difficult to estimate exactly whether each 80-m level is above or below $z_{rev}$, and consequently whether the 80-m hourly trend would follow the surface trend or a reversed pattern.

[24] A more useful parameter is the ratio of $V(80)$ over $V(10)$, since it reaches its minimum in the early afternoon and is greater at night, even when $z_{rev}$ is above 80 m. This ratio will be hereafter referred to as $\rho(h)$, where h is the hour of the day in LST. To find the best fitting curve for $\rho(h)$, given only its two values at 0000 and 1200 UTC ($\rho_{00}$ and $\rho_{12}$ respectively), an independent observational data set was used, obtained from the Pacific Northwest Laboratory (PNL) and described by *Sandusky et al.* [1982]. These data were collected at several heights (e.g., 9 m, 45 m, and 76 m) at 16 sites for the years 1976–1981 (Table 1), with hourly frequency both at the surface and aloft. A good approximation for $\rho(h)$ appeared to be a sinusoidal curve of the form:

$$\rho(h) = A \times \sin\left[(h - \delta)\frac{\pi}{12}\right] + \bar{\rho}, \qquad (10)$$

where $\bar{\rho}$ is the observed mean value of $\rho$, $A$ is the amplitude (equal to $(\rho_{max} - \rho_{min})/2$, where $\rho_{max}$ and $\rho_{min}$ are the maximum and minimum observed values of $\rho$), and $\delta$ is the time shift necessary for the time of the sine minimum to coincide with the observed time of $\rho_{min}$.

[25] Figures 2d–2f show examples of observed ("Ratio (obs.)") versus sinusoidal ("Sine (obs.)") $\rho$ curves obtained from the PNL data at three different locations. Equation (10) appears to be a satisfactory approximation for the observed ratio $\rho$. Note that $\rho$ is defined as either $V(45)/V(9)$ or $V(76)/V(9)$ in these examples.

[26] Since hourly trends of $V(80)$ were not available in the 2000 data set used in the rest of the paper, several assumptions were necessary to estimate the three parameters $A$, $\delta$, and $\bar{\rho}$, given only the LS extrapolated values of $\rho$ at 0000 UTC ($\rho_{00}$) and 1200 UTC ($\rho_{12}$). Note that $\rho_{00}$ is generally greater than $\rho_{min}$, and conversely $\rho_{12}$ is generally smaller than $\rho_{max}$. First, the time of the minimum varied between 0800 and 1400 LST, being in average at about 1300 LST. It was thus assumed that the minimum occurs at 1300 LST, giving an estimated value of $\delta$ equal to $-5$. Second, since $\rho_{min}$ generally occurs at about 1300 LST, but the closest value $\rho_{00}$ is at 0000 UTC (i.e., 1500–1900 LST), and analogously $\rho_{max}$ does not occur at 1200 UTC (i.e., 0300–0700 LST), an amplification factor $\alpha$ is needed to correctly estimate the amplitude $A$, such that $A = \alpha(\rho_{12} - \rho_{00})$. Several values of $\alpha$

**Table 5.** List of Selected Stations[a]

| Station ID | Station Name | State | Elevation, m | Annual Mean Speed, m/s | Annual Wind Standard Deviation, m/s | Wind Power Class | Annual Mean Wind Power, W/m$^2$ | Annual Power Standard Deviation, W/m$^2$ |
|---|---|---|---|---|---|---|---|---|
| AMA | Amarillo | TX | 1099 | 10.3 | 4.9 | 7 | 1169 | 1899 |
| CAO | Clayton | NM | 1515 | 10.1 | 5.9 | 7 | 1437 | 4093 |
| CDB | Cold Bay | AK | 30 | 13.6 | 8.5 | 7 | 3766 | 7607 |
| CSM | Clinton | OK | 586 | 10.8 | 5.5 | 7 | 1463 | 2455 |
| DDC | Dodge City | KS | 790 | 10.1 | 5.4 | 7 | 1242 | 2414 |
| GCK | Garden City | KS | 881 | 9.9 | 5.6 | 7 | 1304 | 3297 |
| GDP | Pine Springs | TX | 1662 | 14.8 | 8.7 | 7 | 4476 | 8804 |
| HBR | Hobart | OK | 477 | 10.8 | 5.6 | 7 | 1461 | 2233 |
| RSL | Russell | KS | 568 | 10.3 | 5.6 | 7 | 1379 | 3057 |
| SDB | Sandberg | CA | 1377 | 11.2 | 6.3 | 7 | 1900 | 4410 |

[a]Wind speed and power data are calculated at 80 m.

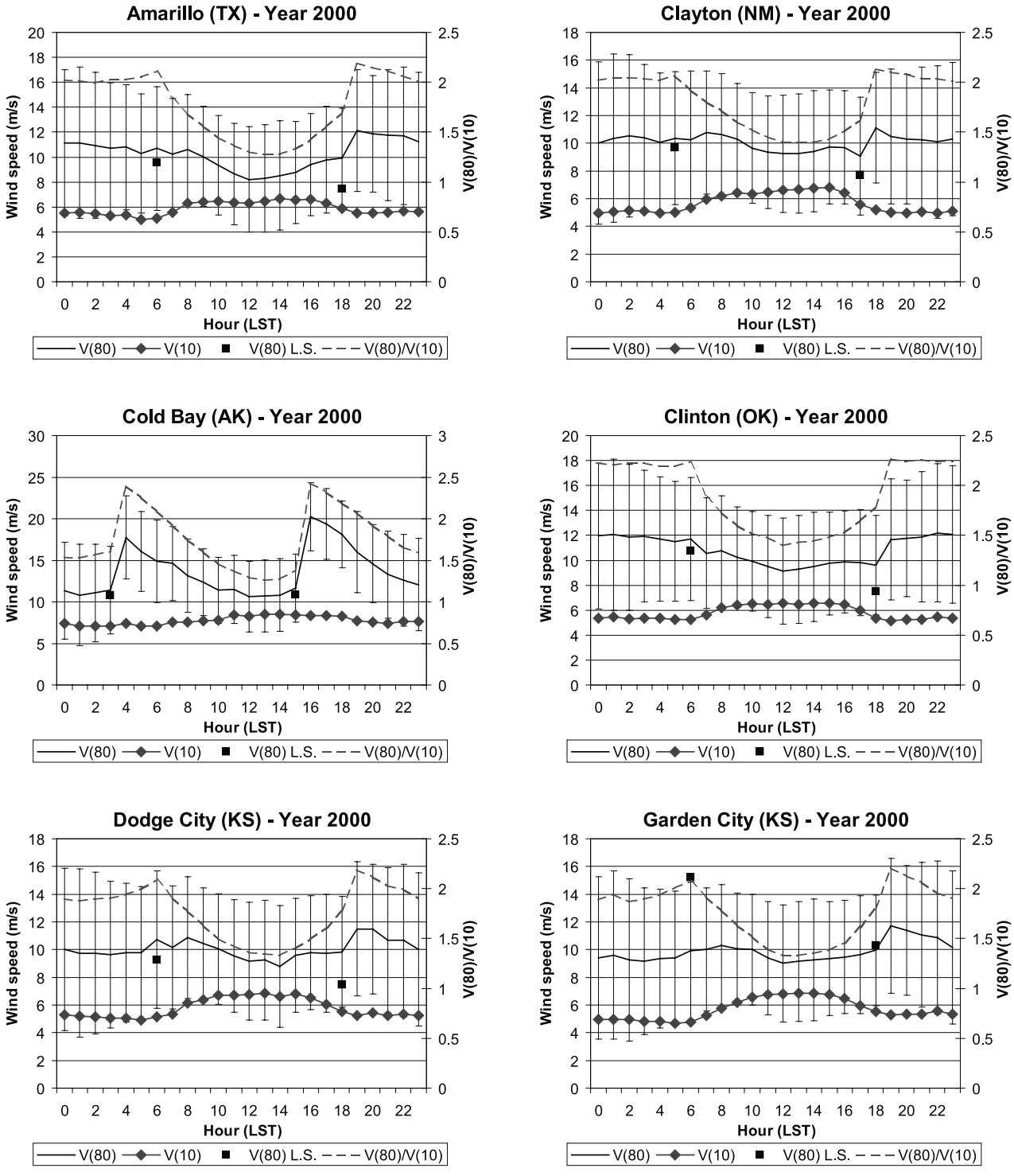


**Figure 4.** Mean and standard deviation of wind speed extrapolated to 80 m at the 10 selected sites, averaged over all days of the year 2000 for each hour of the day. The 10-m mean wind speed and the ratio of 80-m over 10-m mean wind speeds are also shown.

were tested and the corresponding total errors were calculated. It was found that the value of $\alpha$ associated with the lowest total error can vary between 0.9 and 5 at 45 m, and between 0.9 and 1.5 at 76 m, therefore suggesting that $\alpha$ is not as important at ~80 m as it is at 45 m. Since the goal is to find the best $A$ for 80 m, a value of 1.2 was chosen as the best estimate of the amplification factor $\alpha$. Finally, $\bar{\rho}$ was estimated as $(\rho_{12} + \rho_{00})/(2 \times 0.95)$, where 0.95 is the average ratio between $(\rho_{12} + \rho_{00})/2$ and $\bar{\rho}$, based on the PNL data set.

[27] In Figure 2, the curves obtained with the three parameters estimated as described are named "fixed", to remind that both the time of the minimum and the

21562202d, 2003, D9, Downloaded from https://agupubs.onlinelibrary.wiley.com/doi/10.1029/2002JD002076 by CochraneItalia, Wiley Online Library on [10/05/2026]. See the Terms and Conditions (https://onlinelibrary.wiley.com/terms-and-conditions) on Wiley Online Library for rules of use; OA articles are governed by the applicable Creative Commons License

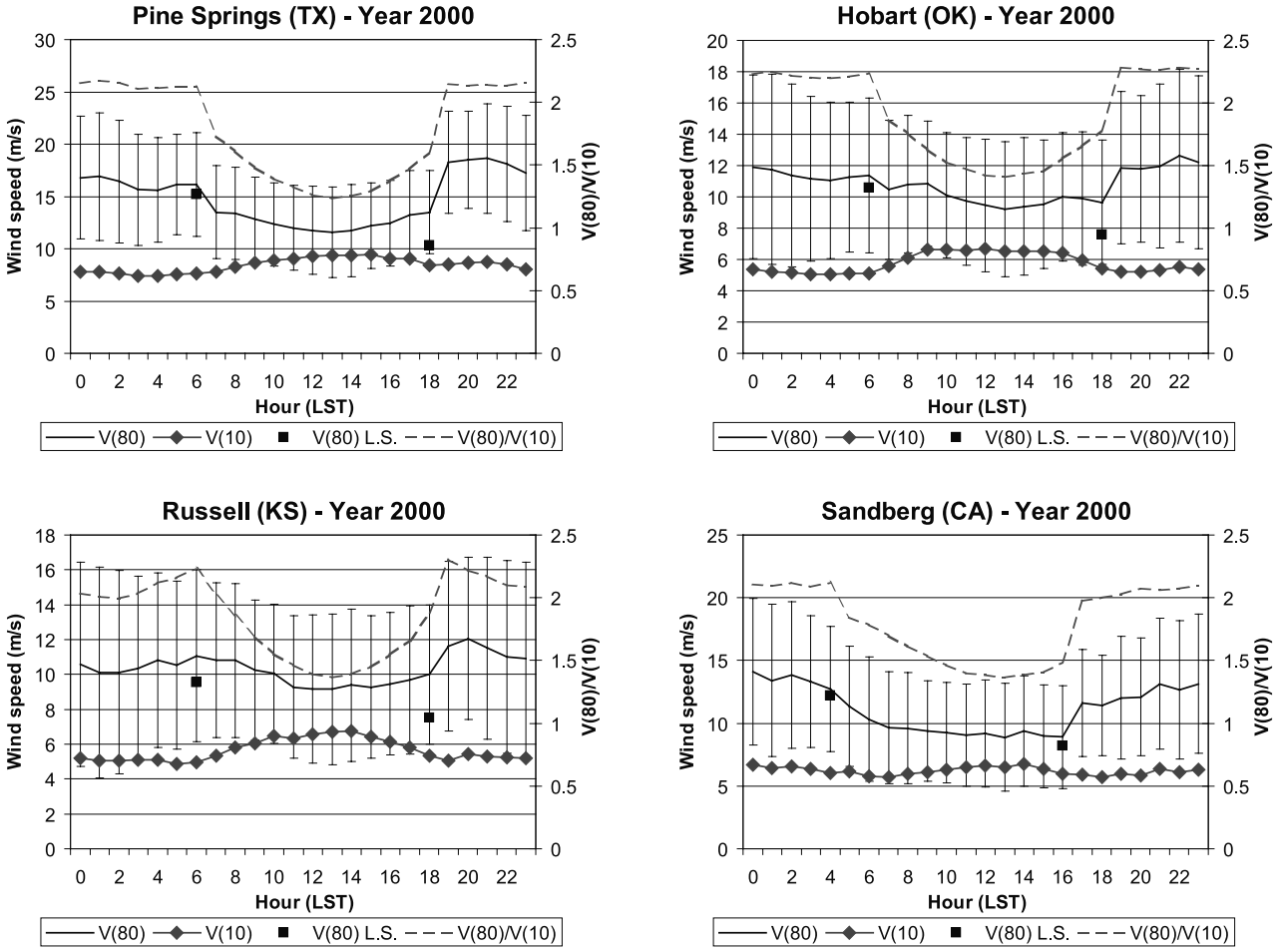


**Figure 4.** (continued)

amplification factor were assumed constant and equal to 1300 LST and 1.2 respectively. Note that this methodology consents to correctly create both hourly trends at 45 m with afternoon peaks (such as Russell, Figure 2a) and hourly trends at 45 m with nighttime maxima (such as Amarillo, Figure 2b), given surface trends with peaks in the afternoon. The figures also show curves (color-coded) obtained with several values of $\alpha$, but the same $A$ and $\delta$. It appears that, the greater $\alpha$, the more likely a surface trend with a maximum during the day will result in a reversed trend at 80 m.

[28] These findings were applied to the 2000 database as follows. For each surface station reporting hourly data, the L.S. values of $V(80)$ were calculated only for those hours for which sounding data were available, i.e., typically at 0000 and 1200 UTC. The corresponding values of $\rho_{00}$ and $\rho_{12}$ were calculated and the corresponding sinusoidal curve $\rho$ with "fixed" parameters (determined as described above) was calculated as well. The hourly trend of $V(80)$ was then estimated by multiplying, at each hour, $V(10)$ by $\rho$.

## 3. Data Analysis

[29] The above methodology was applied to the year 2000 database to generate spatial and temporal distributions and statistics of 80-m wind speeds. For the spatial distribution, daily averages were used, whereas hourly averages were used for studying the temporal evolutions.

### 3.1. Spatial Distribution

[30] The first step in the data analysis was to calculate yearly mean wind speeds at 80 m for all U.S. sounding and surface stations. Previously, the Pacific Northwest Laboratory produced an annual-average map of U.S. wind power (at 10 or 50 m), by interpolating data from about 3500 stations [*Elliott et al.*, 1986]. Data were obtained from several sources, including the National Climatic Data Center and the U.S. Forest Service, and for a variety of years, depending on station data availability. In mountainous regions (elevation greater than 300 m), interpolations were performed based on upper-air climatologies from 1959 for the 850-, 700-, and 500-mb levels [*Elliott et al.*, 1986]. For most locations, vertical interpolations to 10 or 50 m were obtained with the 1/7 friction coefficient power law (i.e., equation (1)). That map represents so far the most complete work on yearly-averaged wind power in the United States.

[31] Although the climatological approach used by *Elliott et al.* [1986] is necessary to evaluate wind potential, it is also useful to look at more recent data (some of which are obtained by newer, more reliable instruments), at raw data (without any horizontal interpolation or assumption), at 80-m rather than 50-m data since wind turbines are now larger,

215622024, 2003, D9, Downloaded from https://agupubs.onlinelibrary.wiley.com/doi/10.1029/2002JD002076 by CochraneItalia, Wiley Online Library on [10/05/2026]. See the Terms and Conditions (https://onlinelibrary.wiley.com/terms-and-conditions) on Wiley Online Library for rules of use; OA articles are governed by the applicable Creative Commons License

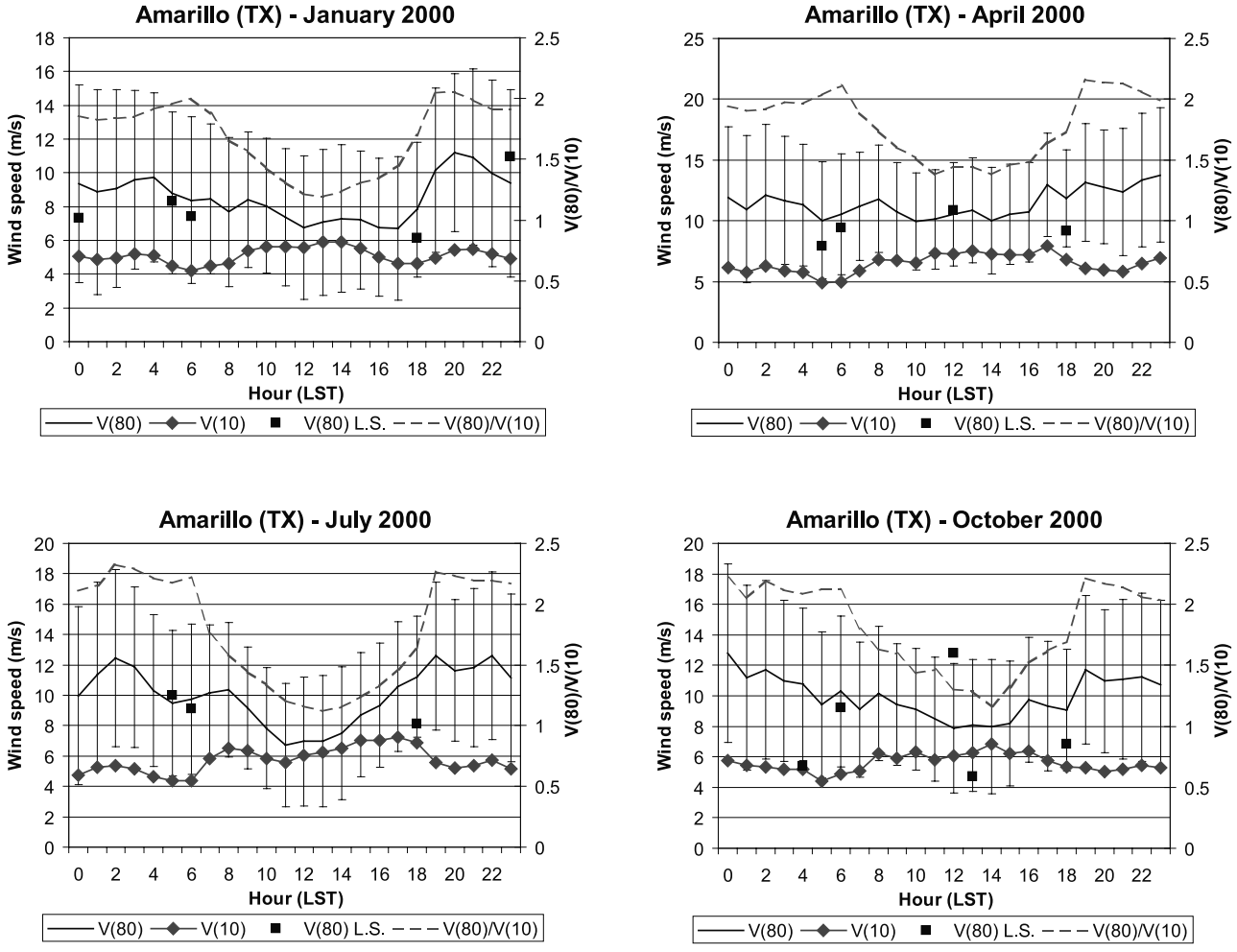


**Figure 5.** Mean and standard deviation of wind speeds extrapolated to 80 m at Amarillo, Texas (AMA), averaged over all days of each month of the year 2000 for each hour of the day. The 10-m mean wind speed and the ratio of 80-m over 10-m mean wind speeds are also shown.

and at elevated winds derived from a combination of soundings and surface measurements. For these reasons, a map with annual mean 80-m wind speeds from U.S. sounding and surface stations was derived here. Figure 3 shows the resulting map for the continental U.S. and offshore sites. Mean speeds at 80 m were separated into seven wind power classes, as defined in Table 1. Figures for Alaska and Hawaii are given in supplemental information available at http://www.stanford.edu/group/efmh/winds.html.

[32] Figure 3 shows statistics only for locations at which measurements were available. Since wind speeds can change over relatively short distances, a fast wind speed at one location does not necessarily mean the wind speed will be fast a few kilometers away. Likewise, the lack of wind measurements in, for example, Maine, does not mean that wind speeds in Maine are generally slow. Wind-farm developers may be able to use Figure 3 to search for general areas where winds may be fast, but additional measurements at the individual site of the proposed farm are necessary to determine better the wind conditions there. However, for analysis purposes, it is assumed here that each station is representative of an area comparable with that of a wind farm.

[33] Figure 3 shows that most of the continental United States experienced wind speeds <6.9 m/s at 80 m (classes 1–2 at 80 m, not suitable for wind farms). Wind power classes at 10 and 80 m are described in Table 2. However, several areas offer appreciable wind power potential. Approximately 24% of the U.S. stations were characterized by mean annual wind speeds ≥6.9 m/s (class 3 or higher at 80 m). At these speeds, the direct cost of electric power from a large 1.5 MW, 77-m modern wind turbine compares with those from a new natural gas or coal power plant (see section 1). As such, the unexploited electric power potential from winds in the United States appears enormous.

[34] Of the class 3 or higher wind stations, 22% (Table 3) were coastal/offshore, distributed mainly along the southeastern and southern coasts. In fact of all coastal/offshore wind stations in North Carolina, Louisiana, and Texas, 60%, 50%, and 89% were in class 3 or higher, respectively. This great reservoir of wind power was not previously identified by *Elliott et al.* [1986], who show winds in these regions (except off the coast of Texas and the northern part of North Carolina), entirely in class 2 (5.9–6.9 m/s at 80 m). Overall, 37% of the U.S. coastal/offshore sites were in class 3 or higher.

[35] The five states with the highest percentage of class 3 or higher stations were Oklahoma, South Dakota, North Dakota, Kansas, and Nebraska (Table 3). Those with the

215622024, 2003, D9, Downloaded from https://agupubs.onlinelibrary.wiley.com/doi/10.1029/2002JD002076 by CochraneItalia, Wiley Online Library on [10/05/2026]. See the Terms and Conditions (https://onlinelibrary.wiley.com/terms-and-conditions) on Wiley Online Library for rules of use; OA articles are governed by the applicable Creative Commons License

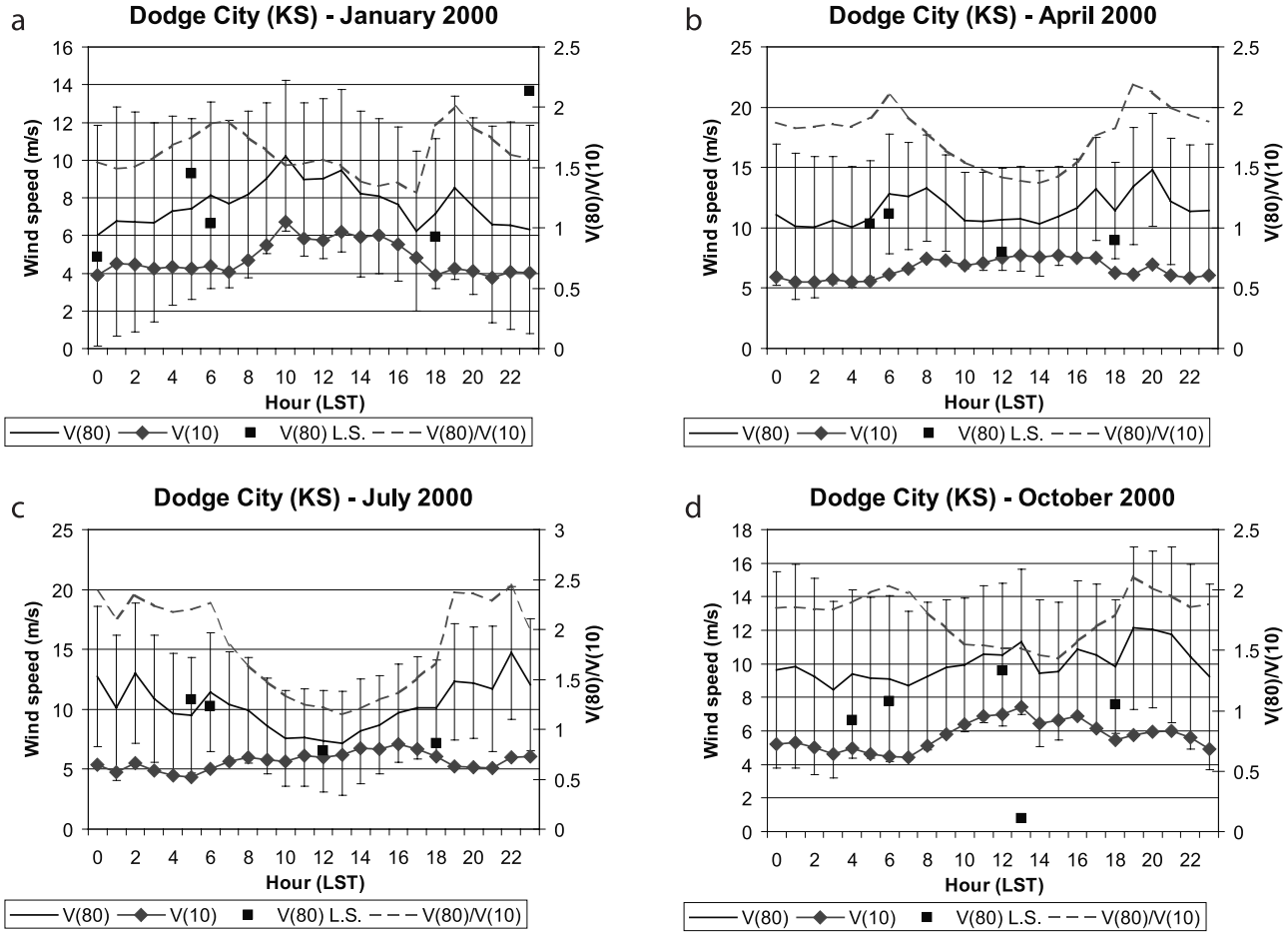


**Figure 6.** (a–d) Same as Figure 5, but for Dodge City, Kansas (DDC).

highest number of class 3 or higher stations were Texas, Alaska, Kansas, Nebraska, Oklahoma, and Minnesota. *Elliott et al.* [1986] found that North Dakota was almost entirely in class 4 (7.5–8.1 m/s at 80 m) or higher. Here, it is found that 64% of stations in North Dakota are in class 4 or higher and 82% are in class 3 or higher. In a recent re-mapping study of the Midwest, *Schwartz and Elliott* [2001] similarly found somewhat less wind power in North Dakota than originally found by *Elliott et al.* [1986]. The highest mean speed at 80 m (23.3 m/s) was at Mount Washington (NH). In Alaska, eight stations had annual mean winds $\geq$9.4 m/s (class 7), three of which were on small islands or oil platforms. Hawaii had one station (Lahaina) with winds in class 5.

[36] Surface and sounding stations were also grouped into eleven regions, described by *Elliott et al.* [1986].

[37] Table 4 lists the number of stations falling into each wind speed class for each region. The North-Central region (Nebraska, Iowa, Minnesota, South and North Dakota), had the highest percent (50.3%) of stations in class 3 or higher, followed closely by the South-Central region (Arkansas, Kansas, Louisiana, Oklahoma, Texas, and Missouri) (46.8%). If it can be assumed that the stations in each region are representative of the region, then these two regions have the greatest wind power potential in the United States in terms of land area.

[38] Figure 3 also shows an area of relatively high mean speeds in the Great Plains region (comprising Texas, Kansas, and Oklahoma), one of the greatest land-based sources of wind energy. This area will be analyzed in greater detail in the next sections, to evaluate diurnal and monthly variations of wind speeds and wind speeds and power averaged over different areas.

### 3.2. Means and Standard Deviations

[39] Ten stations were selected for a detailed statistical analysis. They were chosen based on two criteria: availability of hourly data in the NCDC data set and high wind speed potential (i.e., mean-annual 80-m wind speeds at least in class 3, the minimum recommended for operational wind farms). Surface raw data generally included hourly wind speeds, but in some cases a station reported more than one measurement in an hour, increasing the number of observations in a day to more than 24. In such cases, an average of all values reported for the same hour was used. In addition, hourly raw data were reported in knots (1 knot = 0.515 m/s), and wind speeds of 2 knots (1.03 m/s) or less were generally reported as zero. A value of 1 knot, i.e., an average between 0 and 2 knots, was used to replace all hourly wind speed values reported as zero when extrapolations to 80 m were performed. No such substitution was applied when 10-m wind speed statistics were calculated.

[40] Table 5 lists the stations, their mean-annual 80-m speeds and power output, and the standard deviations of their mean-annual wind speeds and power output. Since

215622024, 2003, D9, Downloaded from https://agupubs.onlinelibrary.wiley.com/doi/10.1029/2002JD002076 by CochraneItalia, Wiley Online Library on [10/05/2026]. See the Terms and Conditions (https://onlinelibrary.wiley.com/terms-and-conditions) on Wiley Online Library for rules of use; OA articles are governed by the applicable Creative Commons License

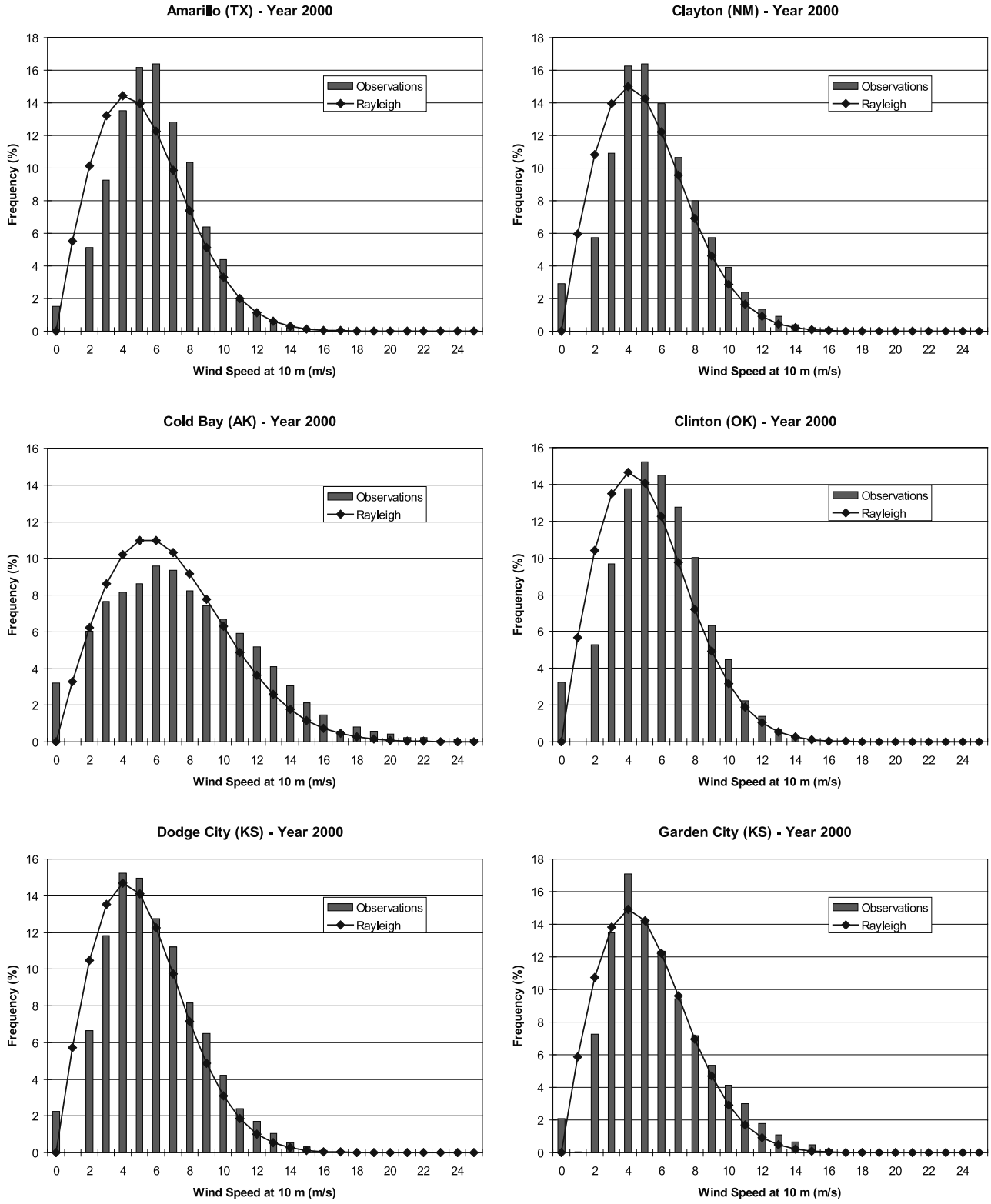


**Figure 7.** Measured (blocks) and Rayleigh (line) wind speed frequency distributions (at 10 m) calculated for all hours of the year 2000 for the 10 selected stations.

these values were calculated from hourly data, some inconsistencies may be found while comparing them with Figure 3, in which values were obtained from daily averages (e.g., CAO is in class 7 in Table 5 but in class 6 in Figure 3). For each station, the 80-m mean-annual wind speed and its standard deviation were calculated for each hour of the day (Figure 4). Since in the rest of the paper all hours will refer to Local Standard Time (LST), the specification "LST" will be omitted hereafter. The 80-m monthly mean wind speed and its standard deviation were also calculated for

215622024, 2003, D9, Downloaded from https://agupubs.onlinelibrary.wiley.com/doi/10.1029/2002JD002076 by CochraneItalia, Wiley Online Library on [10/05/2026]. See the Terms and Conditions (https://onlinelibrary.wiley.com/terms-and-conditions) on Wiley Online Library for rules of use; OA articles are governed by the applicable Creative Commons License

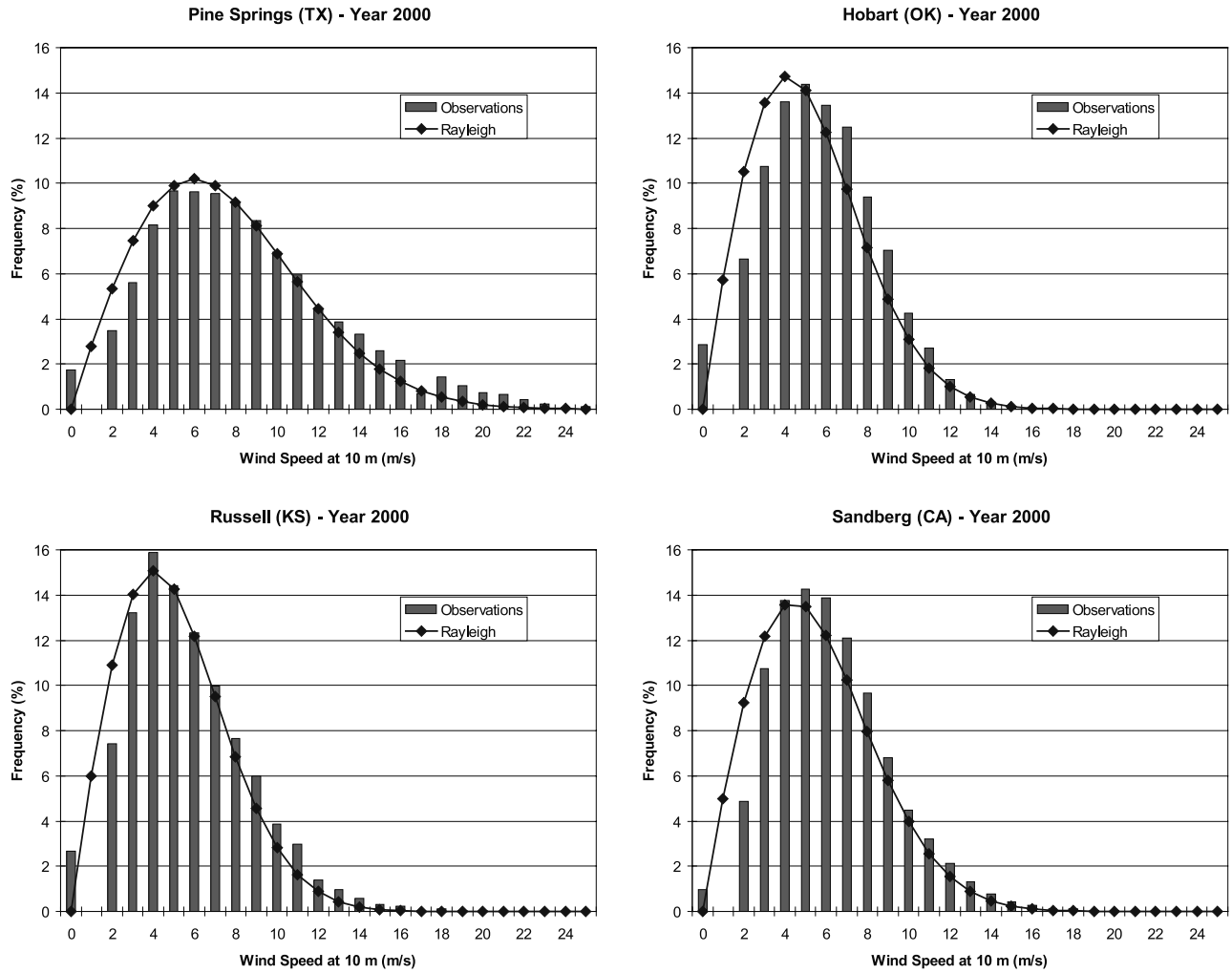


**Figure 7.** (continued)

each hour of the day (e.g., Figures 5 and 6 for two selected stations).

[41] The statistics suggest that the wind speed at a given hour, averaged over either a year or a month, is a fairly steady parameter. Figures 4 and 5 show that the monthly mean for a given hour was within −45% and +60% of the annual mean for that hour. For example, the mean-annual 80-m wind speed at Amarillo (AMA) at 1700 was 9.8 m/s (Figure 4, first graph). Figure 5 shows that the lowest mean speed at 1700 was 6.7 m/s in January, 32% less than the annual mean at that hour. The highest mean speed at that hour was 12.9 m/s in April (32% greater than the annual mean). High variability of the monthly mean at Amarillo occurred in March (Figure 5), when the monthly mean wind speed was 10.0 m/s. The highest mean speed for an individual hour during that month was 12.6 m/s at 1900 (26% greater than the monthly mean), and the lowest mean was 6.7 m/s at 1100 (33% lower than the monthly mean). For Dodge City (DDC), the greatest variability occurred in July (Figure 6), when the monthly mean speed was 10.2 m/s, the highest mean was 14.7 m/s at 2300 (44% of the monthly mean), and the lowest mean was 7.2 m/s at 1300 (29% lower than the monthly mean).

[42] Second, mean wind speed at 80 m was generally lower in the early afternoon than during any other time of the day, for the reason explained in Section 2.2. At Dodge City (DDC), for example, the minimum mean speed occurred between 1100 and 1400 in ~60% of the cases, whereas the maximum was more likely to occur either in the evening (50%) or in the morning (42%) (Figure 6). Note, however, that there are cases (such as January for Dodge City in Figure 6a) when the 80-m wind speed trend follows the 10-m wind speed trend, therefore showing a peak in the afternoon. This is due to the non-uncommon case of $z_{rev}$ located below the 80-m level.

[43] Third, at each hour, the standard deviation of the monthly-mean wind speed was generally within −54% and +108% of the annual mean wind speed. The main implication of this result is that 80-m winds in class 3 or higher are suitable for wind power. In fact, by taking 7.2 m/s as the representative value of class 3, the value corresponding to the mean minus the standard deviation is 3.31 m/s (i.e., 7.2−0.54*7.2), which is above the limit for minimum wind power production from most turbines (3 m/s). Another implication is that wind speed (for high annual mean speed stations) is not so intermittent. Under a Rayleigh distribution of winds (discussed in the next section) with standard deviation equal to 54% of the mean, only 16% of the wind speeds fall below 3.31 m/s. Standard deviations for the annual means were, in the worst case, ±68%, whereas

215622024, 2003, D9, Downloaded from https://agupubs.onlinelibrary.wiley.com/doi/10.1029/2002JD002076 by CochraneItalia, Wiley Online Library on [10/05/2026]. See the Terms and Conditions (https://onlinelibrary.wiley.com/terms-and-conditions) on Wiley Online Library for rules of use; OA articles are governed by the applicable Creative Commons License

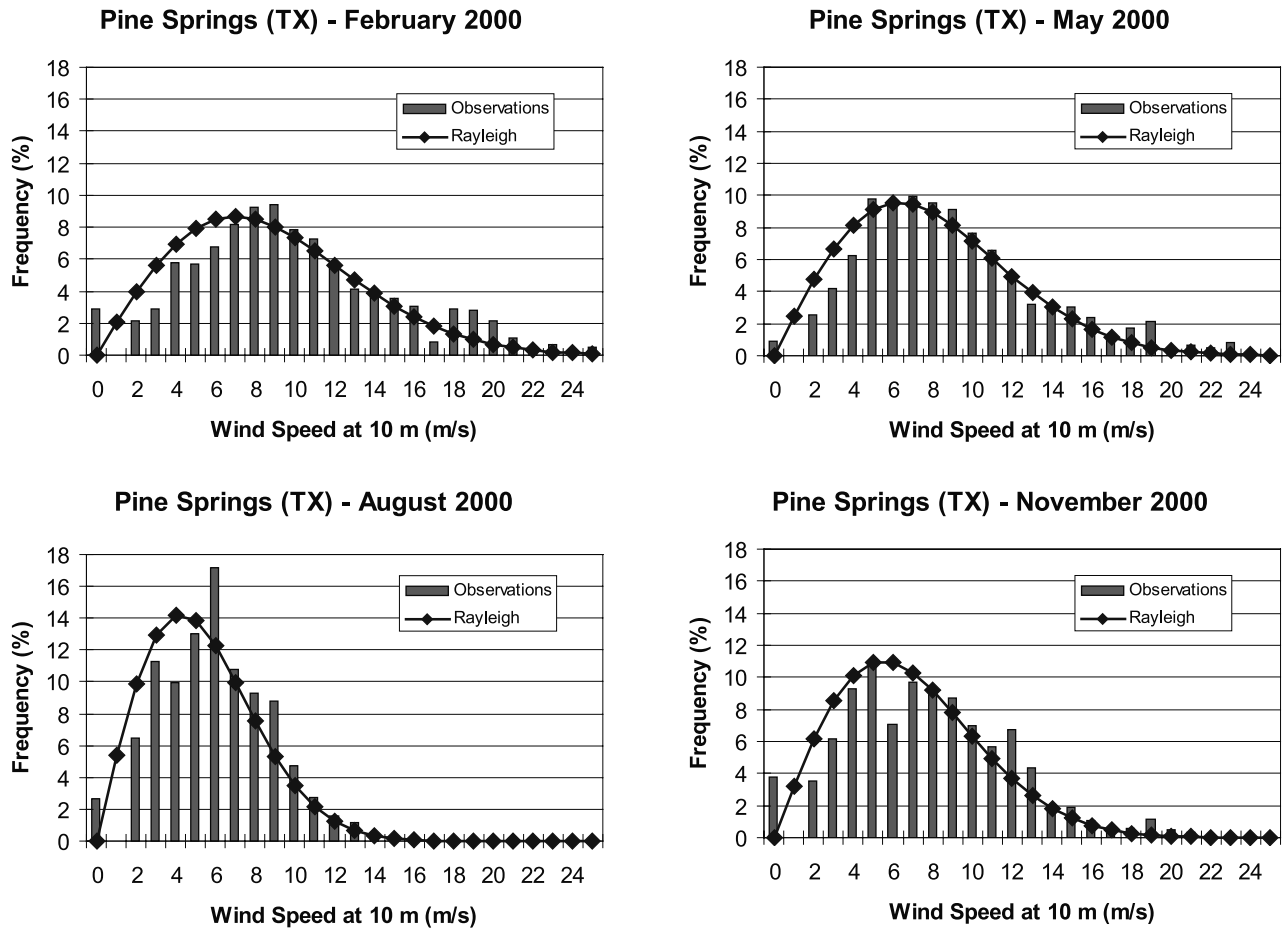


**Figure 8.** Measured (blocks) and Rayleigh (line) wind speed frequency distributions (at 10 m) calculated for all hours of each month of the year 2000 for Pine Springs, Texas (GDP).

standard deviations for the monthly means reached ±94%. This confirms that, the longer the averaging time, the more consistent the wind, i.e., the lower the standard deviation.

### 3.3. Wind Speed Frequency Distributions

[44] In order to evaluate the prevalence of low wind speed events, frequency distributions of winds speeds at 10 m were calculated. Ten-meter distributions were preferred over 80-m distributions for this analysis to eliminate uncertainties arising from vertical extrapolation. Furthermore, since the effect of surface friction decreases rapidly with height, the probability of low speed events is lower at 80 m than it is at 10 m. As a consequence, studying the frequency at 10 m instead of 80 m represents a conservative approach. Winds were divided into 26 speed categories, from 0 to 25 m/s. If a speed was less than 0.5 m/s, the datum was assigned 0 m/s. If it was greater than or equal to 0.5 m/s and lower than 1.5 m/s, it was assigned 1 m/s, and so on. The last category (25 m/s) included all speeds that were greater than or equal to 24.5 m/s. The frequency of each wind speed category was then calculated (as a percentage of the total number of observations) for each station and compared with a theoretical Rayleigh probability density function, calculated as

$$f(v) = \frac{2v}{c^2} \exp\left[-\left(\frac{v}{c}\right)^2\right], \tag{11}$$

where $v$ is wind speed (m/s) and $c$ is $2\bar{v}/\sqrt{\pi}$ (where $\bar{v}$ is the mean wind speed in m/s) (e.g., G. M. Masters, Wind power systems, in *Electric Power: Renewables and Efficiency*, chap. 6, textbook in preparation, 2003). The Rayleigh distribution is a special case of the more general Weibull probability distribution function:

$$f(v) = \frac{k}{c}\left(\frac{v}{c}\right)^{k-1} \exp\left[-\left(\frac{v}{c}\right)^{k}\right], \tag{12}$$

where $k$ is the shape parameter and $c$ is the scale parameter. For $k = 1$, equation (12) looks like an exponential decay, therefore suitable for low speed cases; for $k = 2$, it becomes the Rayleigh distribution described in equation (11), generally used for locations where winds are fairly consistent but with periods of higher speeds (such as at the 10 selected stations); for $k = 3$, the Weibull distribution looks like a bell-shaped function, thus better suitable for locations where winds blow all the time at a fairly constant speed.

[45] Figure 7 compares the measured with theoretical frequency distribution of the winds for all hours of the year 2000 at the 10 selected stations. The Rayleigh curves closely follow the observed distributions for most stations, especially for Dodge City and Pine Springs. Since all wind speeds <3 knots (1.55 m/s) were classified as 0 in the original data set, an unrealistic spike is present in all plots at

215622024, 2003, D9, Downloaded from https://agupubs.onlinelibrary.wiley.com/doi/10.1029/2002JD002076 by CochraneItalia, Wiley Online Library on [10/05/2026]. See the Terms and Conditions (https://onlinelibrary.wiley.com/terms-and-conditions) on Wiley Online Library for rules of use; OA articles are governed by the applicable Creative Commons License

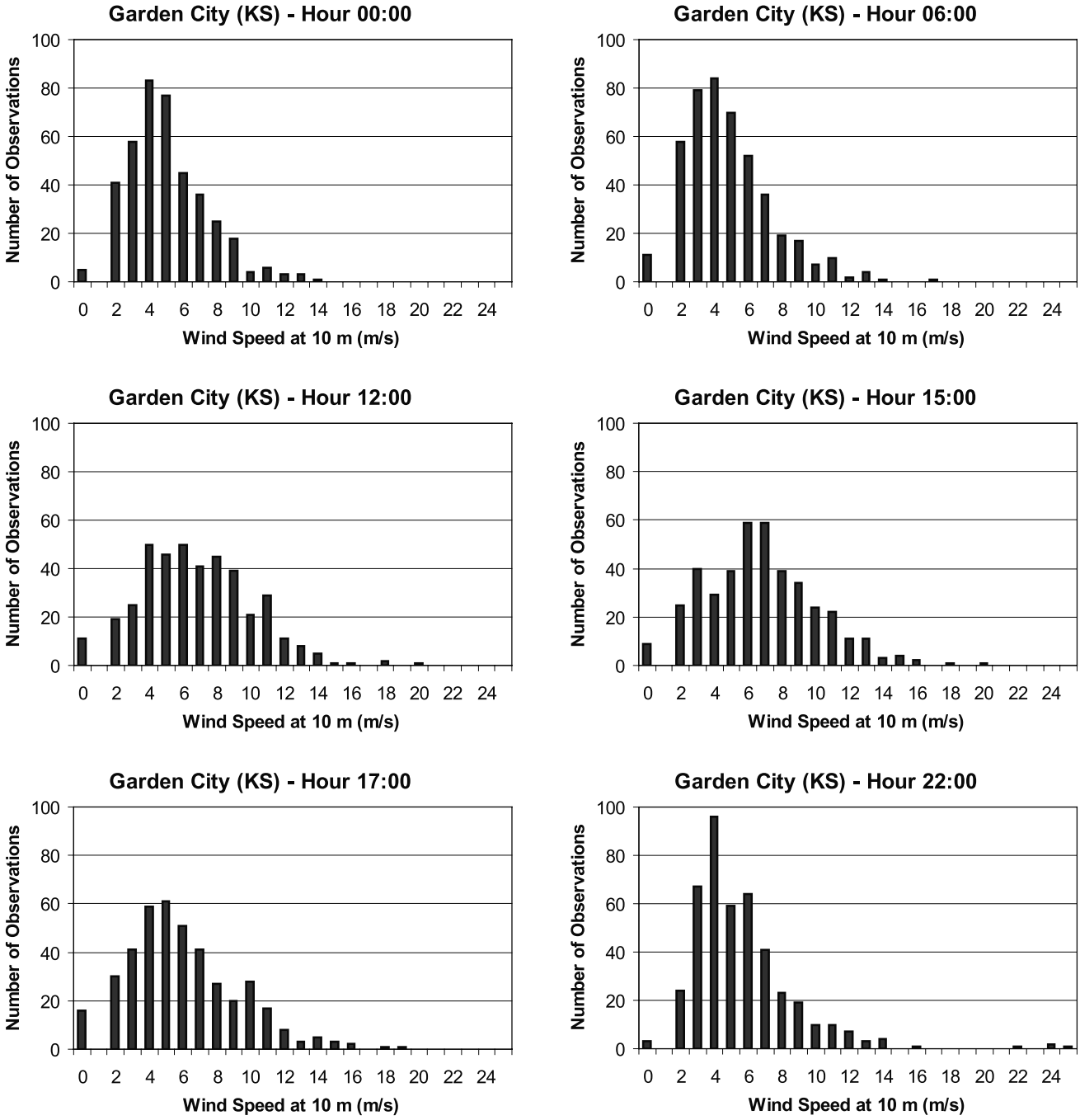


**Figure 9.** Wind speed frequency distributions (at 10 m) calculated for all days of the year 2000 at selected hours of the day for Garden City, Kansas (GCK).

0 wind speed. The frequency of calm winds (wind speeds <2 m/s) ranged from 0.9% at Sandberg to 3.2% at Clinton. The frequency of speeds <3 m/s ranged from 5.2% at Pine Springs to 10.0% at Russell. Figure 8, which shows the frequency distribution by month at Clayton, indicates that low wind speed events tended to occur in the winter rather than in the summer. The greatest frequency of wind speeds <2 m/s at Clayton were in December (7.7%) and January (5.3%).

[46] Hourly frequency distributions for the whole year were calculated to determine if low wind speed events occurred preferentially at specific hours. Results suggest that such events could occur at any hour of the day, but with a slightly higher frequency at night. Figure 9 shows that, at Garden City, for example, the frequency of calm winds varied from a minimum of 0.7% at 2200 to a maximum of 3.9% at 1700. The frequency of the fastest winds was greatest from 1400 to 1600 in the afternoon.

[47] In summary, low wind speed events (<3 m/s at 10 m) were infrequent, occurring less than 10.1% of the total hours of the year in the worst case. Such events were more frequent in winter than in summer.

### 3.4. Wind Power Distributions

[48] Although wind speed statistics are useful, wind power statistics are more relevant for determining energy

215622024, 2003, D9, Downloaded from https://agupubs.onlinelibrary.wiley.com/doi/10.1029/2002JD002076 by CochraneItalia, Wiley Online Library on [10/05/2026]. See the Terms and Conditions (https://onlinelibrary.wiley.com/terms-and-conditions) on Wiley Online Library for rules of use; OA articles are governed by the applicable Creative Commons License

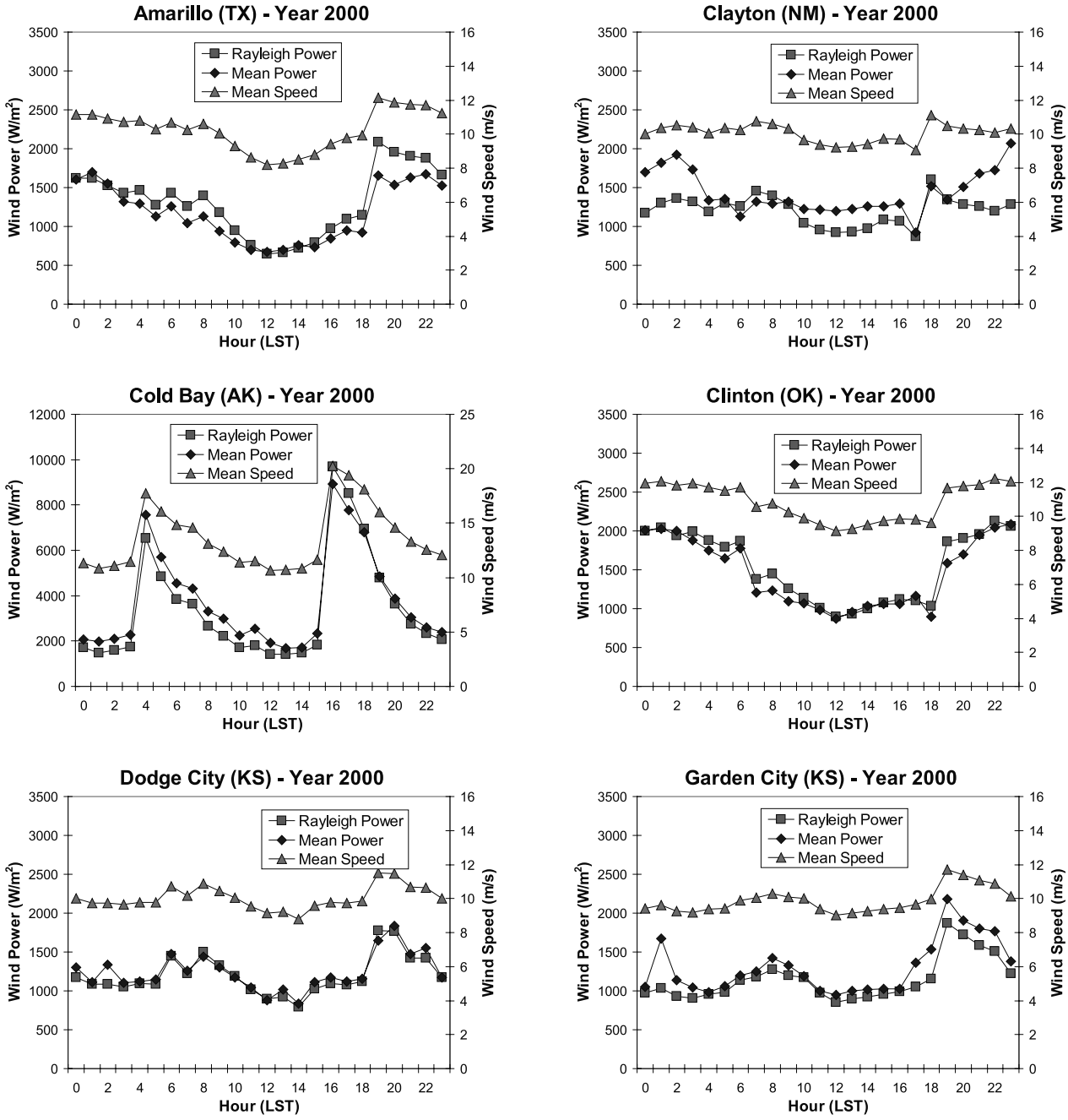


**Figure 10.** Calculated power (diamonds), Rayleigh power (squares), and mean wind speed (triangles) extrapolated to 80 m, averaged over all days of the year 2000 for each hour of the day at the 10 selected sites.

production from wind turbines. Wind power (per rotor area) was therefore calculated for all stations from:

$$P = \frac{1}{2}\rho A v^3, \tag{13}$$

where $\rho$ is the near-surface air density (estimated at 1.225 kg/m$^3$) and A is the rotor area. Observed wind power was compared with theoretical Rayleigh wind power. Figure 10 shows measured wind speed and wind power and Rayleigh wind power at 80 m, averaged over all days of the year 2000 for each hour of the day at the 10 selected stations. As did the maximum annual-averaged hourly wind speed, the minimum annual-averaged hourly wind power occurred during the day/afternoon rather than the night. Figure 10 shows that observed power curves followed the theoretical curves closely, further suggesting that winds are intrinsically Rayleigh in nature. As a consequence, by assuming a Rayleigh distribution, one can calculate the mean power $\bar{P}$ produced at a station as a function of the mean wind speed $\bar{v}$ only (i.e., without needing hourly data) as follows:

$$\bar{P} = \frac{1}{2}\frac{6}{\pi}\rho A \bar{v}^3. \tag{14}$$

215622024, 2003, D9, Downloaded from https://agupubs.onlinelibrary.wiley.com/doi/10.1029/2002JD002076 by CochraneItalia, Wiley Online Library on [10/05/2026]. See the Terms and Conditions (https://onlinelibrary.wiley.com/terms-and-conditions) on Wiley Online Library for rules of use; OA articles are governed by the applicable Creative Commons License

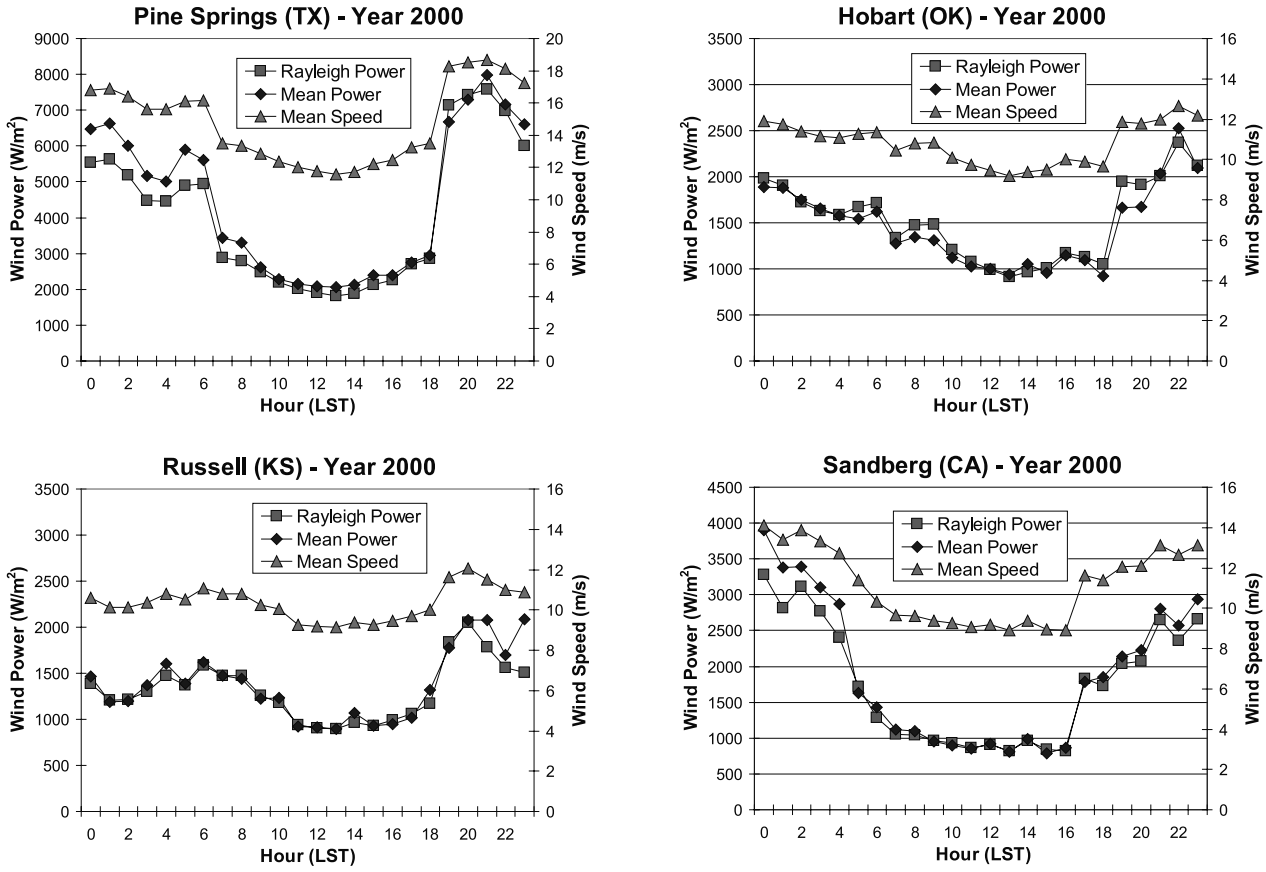


**Figure 10.** (continued)

Figure 11 shows measured wind speed and wind power and Rayleigh wind power at 80 m, averaged over all days of selected months for each hour at Clinton (CSM). The monthly average wind power was maximum in September (1813 W/m$^2$) and minimum in November (908 W/m$^2$). Three other stations (AM, DDC, and GCK) showed maximum power in April and two (CAO, and CDB) had maxima in February (not shown). Five stations out of ten showed minimum power in January, and two in August. Summer months were characterized by fewer low wind speed events, but ironically also lower wind power output than winter months. Late winter months, characterized by more frequent low wind speed events, experienced higher average wind speeds and therefore higher wind power production than summer months. A generic explanation for this is that, since the Northern Hemisphere winter is characterized by a series of extra-tropical cyclones, periods of stormy and windy weather followed by fair and calm weather are common. Due to the greater frequency and strength of synoptic high-pressure systems, fewer extra-tropical storms occur in the summer than in winter.

[49] Because wind power is proportional to the third power of the wind speed, mean annual wind power varied proportionately more than did the mean annual wind speed at the 10 sites compared (Table 5). Figure 11, for example, shows that, at Clinton, the 80-m monthly mean speed at a given hour oscillated between a minimum of 7.3 m/s (August at 1300) and a maximum of 15.9 m/s (August at 2300), corresponding to 67% and 147% of the yearly mean wind speed over all hours of all months (10.8 m/s), respectively. The minimum and maximum wind powers were 338 and 3716 W/m$^2$, corresponding to 23% and 231% of the yearly mean power (1461 W/m$^2$), respectively.

[50] Table 5 shows that the standard deviation of the annual wind power exceeded the annual mean wind power at all sites shown. Since wind power can not be negative, this result suggests that high wind speed tails of the Rayleigh distribution (e.g., Figures 7–8) have a larger influence on the standard deviation of wind power than do calm wind events.

### 3.5. Variation of Wind Power With Number of Wind Farms

[51] Raw data for this study were measured at individual stations. Wind farms contain many turbines spread over large areas. When multiple turbines or multiple wind farms are considered, the area of interest expands. Several studies have shown that, with an increasing number of turbines at a single wind farm, the stability of wind power generation increases [e.g., *Hirst*, 2001; *Hudson et al.*, 2001]. The same should hold true if the number of wind farms increases. To investigate this hypothesis, a comparison of power output averaged over one, three, and eight stations was performed. The first station was DDC, in Kansas. In the three-station case, the stations were DDC, RSL, and GCK, all in Kansas and spread over an area of about 160 $\times$ 120 km$^2$. In the eight-station case, the stations were the previous three plus AMA, GDP, CSM, HBR, and CAO, located in New

215622024, 2003, D9, Downloaded from https://agupubs.onlinelibrary.wiley.com/doi/10.1029/2002JD002076 by CochraneItalia, Wiley Online Library on [10/05/2026]. See the Terms and Conditions (https://onlinelibrary.wiley.com/terms-and-conditions) on Wiley Online Library for rules of use; OA articles are governed by the applicable Creative Commons License

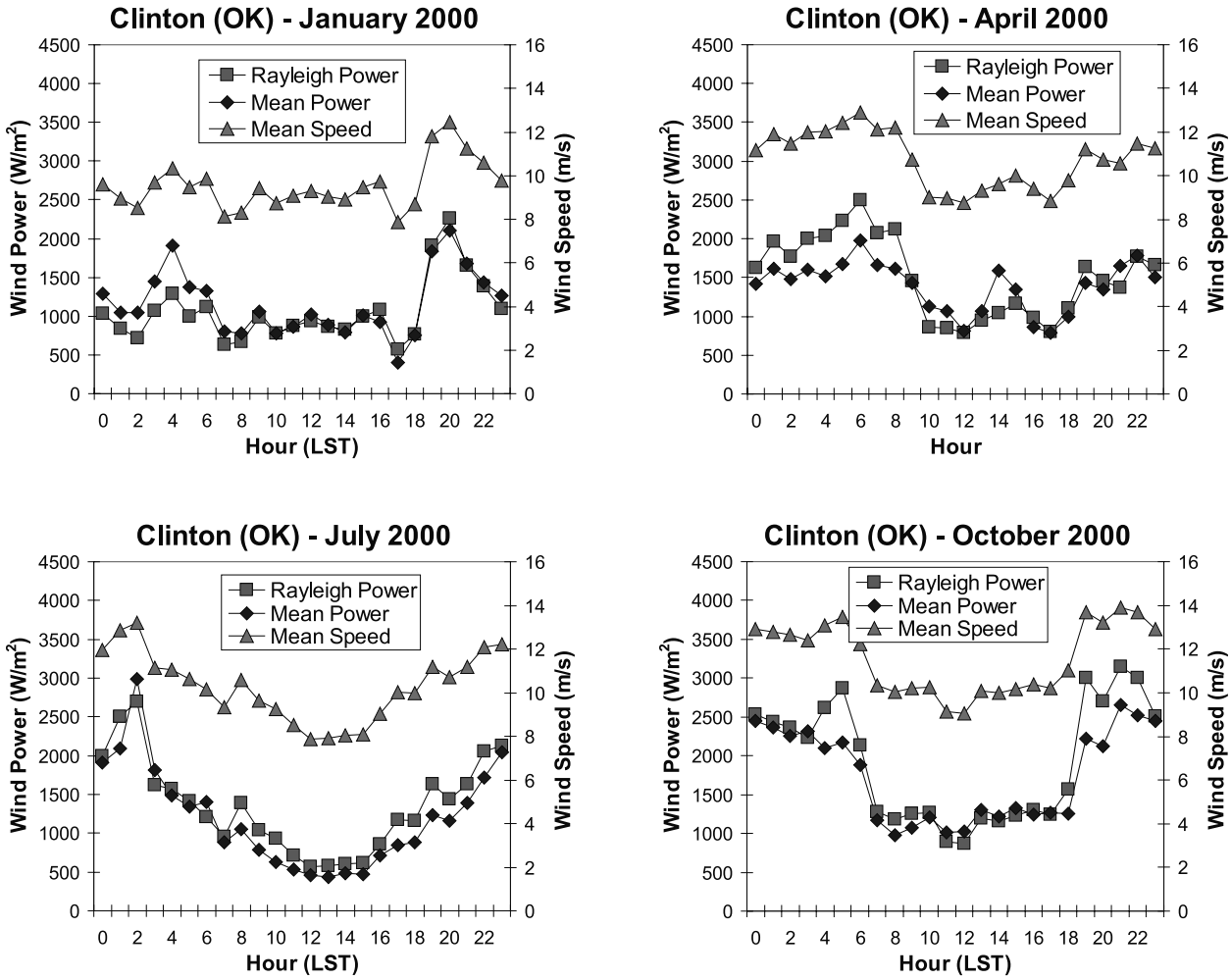


**Figure 11.** Calculated power (diamonds), Rayleigh power (squares), and mean wind speed (triangles) extrapolated to 80 m, averaged over all days of each month of the year 2000 for each hour of the day at Clinton, Oklahoma (CSM).

Mexico, Texas, and Oklahoma. The area covered by the eight stations was approximately 550 × 700 km$^2$.

[52] Since 80-m wind turbines produce little or no power at low wind speeds, care was taken to treat wind speeds <3 m/s, the speed below which no wind power is produced for many turbines. Even when the area-averaged wind speed is lower than 3 m/s, the area-averaged wind power generated by all turbines is not necessarily zero because some turbines may experience wind speeds above 3 m/s, whereas others may experience no winds. To take this into account, a different type of area-averaged wind speed was introduced, named "area-averaged power wind speed" $\underline{V}_p$. First, the area-averaged power $\underline{P}$ at a given hour of a given day was tabulated as

$$\underline{P} = \frac{1}{N}\sum_{i=1}^{N}\frac{1}{2}\rho v_i^3, \tag{15}$$

where $v_i$ is the 80-m wind speed at station $i$ (set to zero if <3 m/s) and $N$ is the number of stations (i.e., 1, 3 or 8). The area-averaged power wind speed $\underline{V}_p$ at a given hour of a given day was then calculated as:

$$\underline{V}_p = \left(\frac{2\underline{P}}{\rho}\right)^{1/3}. \tag{16}$$

Figure 12 shows the frequency distribution of $\underline{V}_p$ for six 4-hour blocks, averaged over the year, for one, three, and eight stations. Several conclusions can be drawn from the figure. First, the larger the averaging area, the lower the probability of a low area-averaged power wind speed. When only one station was considered (Figure 12a), the frequency of the area-averaged power wind speed <3 m/s varied from 3.9% at 0800–1100 to 7.6% at 1200–1500. When three stations were considered (Figure 12b), low power wind speed frequency decreased to 0.4% at 0800–1100 and to 2.6% at 1200–1500. When all eight stations were considered (Figure 12c), the frequency of low-power wind speed became zero. Second, the 2000–2300 and 0000–0300 blocks, depicted with filled squares and circles in Figure 12, had the highest mean and mode, which confirms

21562202d, 2003, D9, Downloaded from https://agupubs.onlinelibrary.wiley.com/doi/10.1029/2002JD002076 by CochraneItalia, Wiley Online Library on [10/05/2026]. See the Terms and Conditions (https://onlinelibrary.wiley.com/terms-and-conditions) on Wiley Online Library for rules of use; OA articles are governed by the applicable Creative Commons License

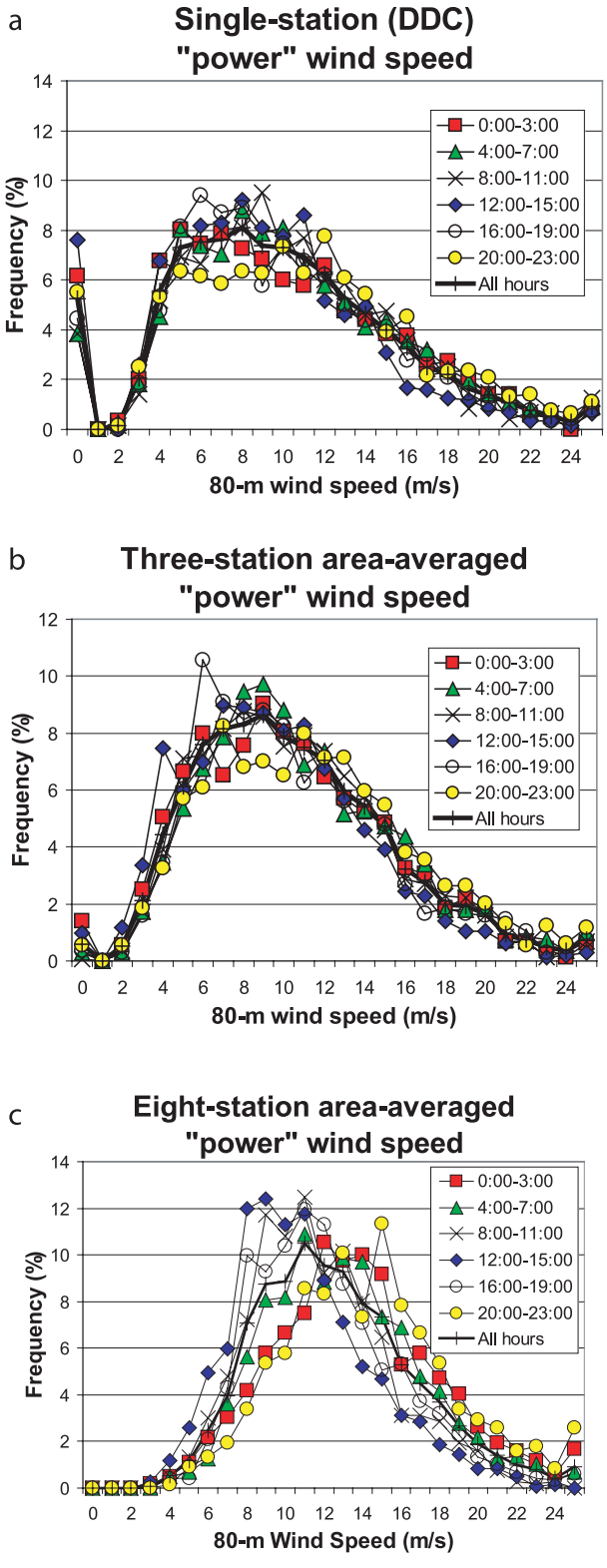


**Figure 12.** Power wind speed distribution, divided into six 4-hour blocks, for (a) one station, (b) three stations, and (c) eight stations.

the previous findings that the greatest wind power occurred at night. The lowest area-averaged power wind speeds in the eight-station case occurred in the morning and afternoon, 0800–1100 and 1200–1500. Finally, the shape of the power wind speed distribution narrowed as the averaging area increased (see, for example, the thicker line, representing an average over all hours, in Figure 12). Therefore the standard deviation of the power wind speed decreased with an increasing averaging area. Furthermore, for the eight station case, a Weibull distribution with $k = 3$ fits the data better than one with $k = 2$ (i.e., a Rayleigh distribution), as expected for locations with constant and high wind speeds.

## 4. Conclusions

[53] In this paper, a methodology for determining 80-m wind speeds given 10-m wind speed measurements was introduced and applied to the United States for the year 2000. The results were analyzed to judge the regularity and spatial distribution of U.S. wind power at 80 m. Conclusions of the study are as follows:

[54] 1. In the year 2000, mean-annual wind speeds at 80 m may have exceeded 6.9 m/s at approximately 24% of the measurement stations in the United States, implying that possibly one quarter of the country is suitable for providing electric power from wind at a direct cost equal to that from a new natural gas or coal power plant.

[55] 2. The greatest previously uncharted reservoir of wind power in the continental United States is offshore and onshore along the southeastern and southern coasts.

[56] 3. The other great wind reservoirs are the north- and south-central regions, charted previously.

[57] 4. The five states with the highest percentage of stations with annual mean 80-m wind speed $\geq$6.9 m/s were Oklahoma, South Dakota, North Dakota, Kansas, and Nebraska.

[58] 5. The standard deviation of the wind speed averaged over multiple locations is less than that at any individual location. As such, intermittency of wind energy from multiple wind farms may be less than that from a single farm, and contingency reserve requirements may decrease with increasing spatial distribution of wind farms.

[59] 6. The minimum wind speed during the year increases when more wind sites are considered. Thus, the probability of no wind power production due to low wind speed events may be greatly reduced (if not eliminated) by a network of wind farms.

[60] 7. Winds are Rayleigh in nature, and actual wind power at any hour of the day during a year is close to Rayleigh wind power.

[61] 8. Because winds, even at a given hour, are Rayleigh in nature, the average wind power over a month at a given hour at a location is a reliable quantity compared with wind power at the same hour, but on any random day of the month. Therefore, requiring turbine owners to produce a summed quantity of energy over a month at a given hour of the day entails little risk once monthly-averaged Rayleigh wind speeds at the given hour and location are known.

[62] 9. Even when the standard deviation of the wind speed is high, the total wind power during an averaging period follows the mean wind speed.

21562202d, 2003, D9, Downloaded from https://agupubs.onlinelibrary.wiley.com/doi/10.1029/2002JD002076 by CochraneItalia, Wiley Online Library on [10/05/2026]. See the Terms and Conditions (https://onlinelibrary.wiley.com/terms-and-conditions) on Wiley Online Library for rules of use; OA articles are governed by the applicable Creative Commons License

[63] **Acknowledgments.** This work was supported by the Environmental Protection Agency, the NASA New Investigator Program in Earth Sciences, the National Science Foundation, and the David and Lucile Packard Foundation and the Hewlett-Packard Company. Data were obtained from National Climatic Data Center, Forecast System Laboratory, and Pacific Northwest Laboratory. We would also like to thank Scott Archer, Gil Master, Paul Veers, Henry Dodd, and Donald Anderson for helpful comments.

## References

Arya, S. P., *Introduction to Micrometeorology*, 307 pp., Academic, San Diego, Calif., 1988.

Bolinger, M., and R. Wiser, Summary of power authority letters of intent for renewable energy, memorandum, Lawrence Berkeley Natl. Lab., Berkeley, Calif., 30 Oct. 2001.

Elliott, D. L., C. G. Holladay, W. R. Barchet, H. P. Foote, and W. F. Sandusky, *Wind Energy Resource Atlas of the United States*, *DOE/CH 10093-4*, Natl. Renew. Energy Lab., Golden, Colo., 1986.

Energy Information Administration (EIA), Table 1. Electric Power Industry Summary Statistics for the United States, 1999 and 2000, in *Electric Power Annual 2000*, vol. 2, p. 11, Off. of Coal, Nucl., Electr. and Alt. Fuels, Washington, D.C., 2001.

Hirst, E., Interactions of wind farms with bulk-power operations and markets, report, Proj. for Sustain. FERC Energy Policy, Alexandria, Va., 2001.

Hudson, R., B. Kirby, and Y.-H. Wan, The impact of wind generation on system regulation requirements, paper presented at AWEA Wind Power Conference, Am. Wind Energy Assoc., Washington, D.C., 3 – 7 June 2001.

Jacobson, M. Z., *Fundamentals of Atmospheric Modeling*, 656 pp., Cambridge Univ. Press, New York, 1999.

Jacobson, M. Z., and G. M. Masters, Exploiting wind versus coal, *Science*, *293*, 1438, 2001.

National Climatic Data Center, Hourly surface data, http://lwf.ncdc.noaa.gov/oa/climate/climatedata.html, Asheville, N.C., 2001.

North American Electric Reliability Council, Generating unit statistical brochure, 1995 – 1999, Princeton, N.J., Oct. 2000.

Office of Fossil Energy, Market-based advanced coal power systems, final report, sect. 9, Dep. of Energy, Washington, D.C., 2001.

Riehl, H., *Introduction to the Atmosphere*, 516 pp., McGraw-Hill, New York, 1972.

Sandusky, W. F., D. S. Renné, and D. L. Hadley, Candidate wind turbine generator site summarized meteorological data for December 1976 through December 1981, *PNL-4407*, Pac. Northwest Lab., Richland, Wash., 1982.

Schwartz, M., and D. Elliott, Remapping of the wind energy resource in the midwestern United States, *NREL/AB-500-31083*, Natl. Renew. Energy Lab., Golden, Colo., 2001.

Steurer, P., Six second upper air data, *TD-9948*, http://www1.ncdc.noaa.gov/pub/data/documentlibrary/tddoc/td9948.pdf, Natl. Clim. Data Cent., Asheville, N.C., 1996.

C. L. Archer and M. Z. Jacobson, Department of Civil and Environmental Engineering, Stanford University, Stanford, CA 94305, USA. (lozej@stanford.edu; jacobson@ce.stanford.edu)

215622024, 2003, D9, Downloaded from https://agupubs.onlinelibrary.wiley.com/doi/10.1029/2002JD002076 by CochraneItalia, Wiley Online Library on [10/05/2026]. See the Terms and Conditions (https://onlinelibrary.wiley.com/terms-and-conditions) on Wiley Online Library for rules of use; OA articles are governed by the applicable Creative Commons License